



VIDEO BASED BEARING INSPECTION

ARDA MOLLAKÖY

SEPTEMBER 2019

VIDEO BASED BEARING INSPECTION

A THESIS SUBMITTED TO
THE GRADUATE SCHOOL OF NATURAL AND APPLIED
SCIENCES OF
ÇANKAYA UNIVERSITY

BY
ARDA MOLLAKÖY

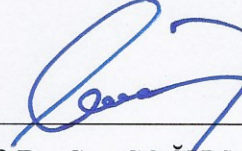
IN PARTIAL FULFILLMENT OF THE REQUIREMENTS FOR THE
DEGREE OF
MASTER OF SCIENCE
IN
THE DEPARTMENT OF
ELECTRONIC AND COMMUNICATION ENGINEERING

SEPTEMBER 2019

Title of the Thesis: **Video Based Bearing Inspection**

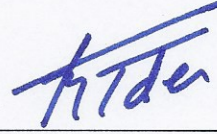
Submitted By **Arda MOLLAKÖY**

Approval of the Graduate School of Natural and Applied Sciences, Çankaya University.



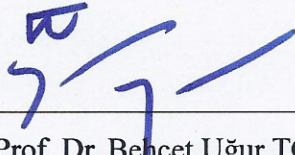
Prof. Dr. Can ÇOĞUN
Director

I certify that this thesis satisfies all the requirements as a thesis for the degree of Master of Science.

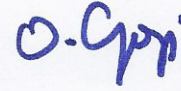


Prof. Dr. Sıtkı Kemal İDER
Head of Department

This is to certify that we have read this thesis and that in our opinion it is fully adequate, in scope and quality, as a thesis for the degree of Master of Science.



Assoc. Prof. Dr. Behçet Uğur TÖREYİN
Co-Supervisor



Assoc. Prof. Dr. Orhan GAZİ
Supervisor

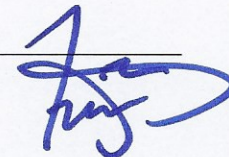
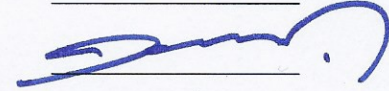
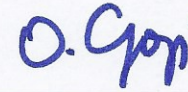
Examination Date: 11.09.2019

Examining Committee Members

Assoc. Prof. Dr. Orhan GAZİ Çankaya Univ.

Dr. Lecturer Göker ŞENER Çankaya Univ.

Dr. Lecturer Cevat RAHEBİ Altınbaş Univ.



STATEMENT OF NON-PLAGIARISM PAGE

I hereby declare that all information in this document has been obtained and presented in accordance with academic rules and ethical conduct. I also declare that, as required by these rules and conduct, I have fully cited and referenced all material and results that are not original to this work.

Name, Last Name: Arda MOLLAKÖY

Signature:



Date: 09.10.2019

ABSTRACT

VIDEO BASED BEARING INSPECTION

MOLLAKÖY, Arda

M.Sc., Department of Electronic and Communication Engineering

Supervisor: Assoc. Prof. Dr. Orhan GAZI

SEPTEMBER 2019, 87 pages

The production of bearings according to the standards directly affects the quality and life of both the bearings and the machines and components (such as gearbox, alternator) in which the bearings are used. Therefore, the final quality control stage in bearing production is of paramount importance. Visual quality control, which is the final stage of the bearing production line, is carried out by the skilled workers under bright light. The performance of quality audits depends on the experience of the auditors and the level of focus during the audit. In order to maintain a high level of focus, workers are employed in short and frequent shifts. However, even experienced workers can see quality control defects due to low focus levels. Consequently, the final product can be sent to the customer as defective.

In order to improve this process and prevent the delivery of defective products, the shift in the visual control phase and thus the increase in the number of workers is a possible solution. However, it is clear that such a solution is not economic. Another option to solve this problem is to develop the machine vision based visual defect control system proposed in this thesis. Although similar systems are widely used in different industries, they are not yet at the desired efficiency in the bearing manufacturing industry.

In this thesis, an image processing based quality control system that works on FPGA platform is developed to help visual quality control.

Keywords: Variance, KLD, Power Graphs, Shifting Rolling Window

ÖZ

VİDEO TABANLI RULMAN KONTROLÜ

MOLLAKÖY, Arda

Yüksek Lisans, Elektronik ve Haberleşme Mühendisliği Anabilim Dalı

Tez Yöneticisi: Doç. Dr. Orhan GAZİ

EYLÜL 2019, 87 sayfa

Standartlara göre rulmanların üretimi, rulmanların kullanıldığı makinelerin ve parçaların (dişli kutusu, alternatör gibi) kalitesini ve ömrünü doğrudan etkiler. Bu nedenle, rulman üretiminde son kalite kontrol aşaması çok önemlidir. Rulman üretim hattının son aşaması olan görsel kalite kontrolü, uzman kişiler tarafından parlak ışık altında gerçekleştirilir. Kalite denetimlerinin performansı, denetçilerin deneyimine ve denetim sırasındaki odak düzeyine bağlıdır. Yüksek seviyede odaklanma sağlamak için, işçiler kısa ve sık vardiyalarda istihdam edilir. Bununla birlikte, deneyimli işçiler bile düşük odak seviyelerinden dolayı kalite kontrol kusurlarını görebilir. Sonuç olarak, nihai ürün müşteriye kusurlu olarak gönderilebilir.

Bu süreci iyileştirmek ve kusurlu ürünlerin teslimatını önlemek için, görsel kontrol aşamasındaki değişiklik ve dolayısıyla çalışan sayısındaki artış olası bir çözümdür. Ancak, böyle bir çözümün ekonomik olmadığı açıktır. Bu sorunu çözmek için başka bir seçenek, bu tezde önerilen makine vizyonuna dayalı görsel hata kontrol sistemini geliştirmek. Her ne kadar benzer sistemler farklı endüstrilerde yaygın olarak kullanılsa da, henüz rulman üretim endüstrisinde istenen verimlilikte değildir.

Bu tezde, görsel kalite kontrolüne yardımcı olmak için FPGA platformunda çalışacak görüntü işleme tabanlı kalite kontrol sistemi geliştirilmektedir.

Anahtar Kelimeler: Varyans, Kullback-Leibler Uzaklığı, Güç Grafikleri, Kayan Pencere.



To My Love...

ACKNOWLEDGEMENTS

The author would like to express sincere gratitude to his supervisor Assoc. Prof. Dr. Orhan GAZİ and co-supervisor Assoc. Prof. Dr. Behçet Uğur TÖREYİN for their encouragement, guidance, valuable support and patience throughout the this study.

The author would also like to express his sincere thanks to Dr. Lecturer Göker ŞENER and Dr. Lecturer Cevat RAHEBİ for accepting to read and review this thesis and providing useful comments.

The author would like to express my deepest thanks to my managers, Dr.-Ing Feridun ÖZHAN, Dr.-Ing Hamdullah MERDANE at Ortadoğu Rulman Sanayi A.Ş. for their support and encouragement. The author would also like to express my gratitude to my colleagues, Kurtuluş TÜFEKÇİ, Şerafettin ŞENER, İsmail Burak KANDEMİR, Kemal ÇETİN, Ersen ÖZÇUBUKÇU, Mesut TEKİN, Yusuf İNANOĞLU and Oğuzhan ÇİFTÇİ on behalf of all Ortadoğu Rulman Sanayi A.Ş. members, for their interest, help and technical assistance. The author is indebted to Türkiye Bilimsel ve Teknik Araştırma Kurumu – Teknoloji ve Yenilik Destek Programları Başkanlığı (TÜBİTAK - TEYDEB) for the financial support under the contract number TEYDEB-3140509.

The author would like to express his thank to Fatih GENÇ for his valuable technical assistance, help and support during this study. The author also would like to express his thank to Dr. Emre YENGEL and Res. Assist. Sibel ÇİMEN for their valuable support and help during this study.

The author is also indebted to his parents, Sevgi MOLLAKÖY, Nizamettin MOLLAKÖY, and his sister Arzu AYCAN for enlightening me with their, inspiration, understanding, endless love, guidance and wisdom through his entire life.

Finally, the author owes his deepest gratitude to his love Selin SULU for her continuous support and patience during this period. I really appreciate for her existence.

XXXXXS
GCPS

TABLE OF CONTENTS

STATEMENT OF NON-PLAGIARISM PAGE	iii
ABSTRACT	iv
ÖZ	v
ACKNOWLEDGEMENTS	vii
TABLE OF CONTENTS	ix
LIST OF FIGURES	xii
LIST OF TABLES	xiv
LIST OF ABBREVIATIONS	xv
CHAPTER 1	1
INTRODUCTION	1
1.1. General Context.....	1
1.2. Main Objectives	2
1.3. Organization of This Thesis	3
CHAPTER 2	5
2.1. Bearing Industry	5
2.1.1. Bearing Manufacturing Process	6
2.2. Quality Control.....	7
2.2.1. Quality Control for Bearings.....	9
2.2.2. Bearing Surface Inspection	10
2.2.2.1. Surface Defects.....	10
2.2.2.2. Current Setup: Manual Visual Inspection.....	13
2.3. Non-Destructive Testing for Surface Inspection.....	14
CHAPTER 3	16
MACHINE VISION BASED BEARING DEFECT DETECTION SYSTEM...	16
3.1. Inspection Requirements and Conditions.....	17
3.2. Camera Selection.....	18
3.2.1. Area Scan or Line Scan	19

3.2.2. Monochrome or Color Camera	21
3.2.3. Sensor Type.....	23
3.2.4. Resolution.....	25
3.2.5. Camera Interface	26
3.3. Lens Selection	27
3.4. Lighting System	28
3.4.1. Lighting Technique	29
3.4.2. Lighting Source	30
3.5. Processing Platform.....	32
3.6. System Design and Installation	34
3.7. Communication between PLC and FPGA.....	38
CHAPTER 4	41
DEFECT DETECTION METHODS	41
4.1. Otsu Thresholding on Grayscale Image	42
4.2. Blob Extraction.....	42
4.3. Crop and Resizing	44
4.4. Hough Transform for Circle Detection	46
4.5. ROI Segmentation	46
4.8. Variance.....	49
4.9. Skewness	49
4.10. Kurtosis	49
4.11. Median Filter	50
4.12. Gaussian Blur	50
4.13. Erosion and Dilation.....	51
4.14. Kullback-Leibler Distance	51
4.15. Shifting Rolling Window	52
CHAPTER 5	54
EXPERIMENTAL RESULTS.....	54
5.1. Adaptive Thresholding	54
5.2. Mean, STD, Skewness, Kurtosis and Variance	55
5.3. KLD Results	56
5.4. Power Graphs Results	57

5.5. Sliding Rolling Window Results	59
5.5.1. Rubber Seal’s Defects	59
5.5.1.1. Overlap on Rubber Seals	59
5.5.1.2. Deformation on Rubber Seals	61
5.5.1.3. Scratch on Rubber Seals	62
5.5.2. Face Defects	63
5.5.2.1. Scratch on Face.....	63
5.5.2.2. Impact on Face	64
5.5.3. Outer Diameter Defects.....	65
5.5.3.1 Rust Defects on Outer Diameter.....	66
5.5.3.2. Shoe Trail Defects on Outer Diameter	68
5.5.3.3. Impact Defects on Outer Diameter	71
5.6. Confusion Matrices	74
CHAPTER 6	78
GENERAL CONCLUSION AND FUTURE WORKS	78
6.1. General Conclusion	78
6.2. FutureWorks	82
REFERENCES	83

LIST OF FIGURES

Figure 1: Bearing components.	7
Figure 2: Visual inspection system “VisiBear”.	34
Figure 3: Physical system with visual inspection system	34
Figure 4: Trigger signals between FPGA and PLC.	39
Figure 5: Design of trigger card, (a) PCB layout, (b) PCB.	40
Figure 6: Detected bearing’s outer ring boundaries coordinates.	43
Figure 7: The effect of applying the 4 and 8 connectivity types.	44
Figure 8: Crop and resize, (a) Original image. (b) Cropped image.	45
Figure 9: CHT result, (a) Cropped image, (b) CHT applied result image.	46
Figure 10: Polar to Cartesian conversation.	47
Figure 11: Image segmentation of bearings, (a) Segmentation results, (b) Outer ring, (c) Rubber Seal, (d) Inner ring.	48
Figure 12: Examples of bearings illuminated with varying light intensities.	54
Figure 13: Relationship between Light Intensity (lux) – Threshold value	55
Figure 14: KLD results, (a) Histogram-PDF graph of reversely assembled seal, (b) Histogram-PDF graph of missing rubber seal, (c) Histogram-PDF graph of properly assembled rubber seal, (d) Normal PDF graphics of these bearing samples.	57
Figure 15: Power graph’s results, (a) Raw data, (b) High-Pass filtered data, (c) Absolute values from High-Pass filtered data, (d) Comparative data with threshold value applied.	58
Figure 16: Overlap defect detection, (a) Bearing sample with Overlap defect, (b) Cartesian coordinates, (c) ROI of defect inspection, (c) Inner rubber seal’s lip, (d) Outer rubber seal’s lip.	60
Figure 17: Deformation defect detection, (a) Bearing sample with deformation defect, (b) Cartesian coordinates, (c) Binary transformation image, (c) Erosion/dilation applied image, (d) ROI of defect inspection.	61
Figure 18: Scratch defect detection, (a) Bearing sample with scratch defect, (b)	

Cartesian coordinates, (c) Binary transformation image, (c) Erosion/dilation applied image, (d) ROI of defect inspection.....	62
Figure 19: Scratch defect detection on face, (a) Bearing sample with scratch defect on inner face, (b) Cartesian coordinates on grayscale, (c) Binary transformation image and also ROI of defect inspection.	63
Figure 20: Scratch defect detection on face, (a) Bearing sample with impact defect on inner face, (b) Cartesian coordinates on grayscale, (c) Binary transformation image and also ROI of defect inspection.	64
Figure 21: Scratch defect detection on face, (a) An exemplary outer diameter bearing image. (b) The brightest parts of the image in question are determined by Otsu thresholding, subjected to expansion morphological processing and marked with the method of connected components to obtain the smallest spanning box.	65
Figure 22: ROI with rust defect on the outside diameter.	66
Figure 23: Gaussian Blur image and median filter are applied on rust ROI.....	67
Figure 24: Binary transformed image on rust ROI.	67
Figure 25: Cropped and resized image on rust ROI for defect detection.	68
Figure 26: 32x32 frame results in a bearing with rust defects on outer diameter.	68
Figure 27: Example of a bearing with shoe trail defect on the outside diameter.	69
Figure 28: ROI with shoe trail defect on the outside diameter.	69
Figure 29: Gaussian Blur image and median filter are applied on shoe trail ROI. ...	70
Figure 30: Binary transformed image on shoe trail ROI.	70
Figure 31: Cropped and resized image on shoe trail ROI for defect detection.....	71
Figure 32: 32x32 frame results in a bearing with shoe trail defects on outer diameter.	71
Figure 33: Cropped and resized image on impact ROI for defect detection.....	72
Figure 34: ROI with impact defect on the outside diameter.	72
Figure 35: Gaussian Blur image and median filter are applied on impact ROI.....	73
Figure 36: Binary transformed image on impact ROI.	73
Figure 37: Cropped and resized image on impact ROI for defect detection.....	74
Figure 38: 32x32 frame results in a bearing with impact defects on outer diameter.	74

LIST OF TABLES

Table 1: List of the main potential defects with their characteristics.....	11
Table 2: Hardware specifications.	35
Table 3: Mathematical results of the defect types of seal.....	56
Table 4: Confusion matrix of the inspection results of the first inspection station..	75
Table 5: Confusion matrix of the inspection results of the second inspection station.	76
Table 6: Confusion matrix of the inspection results of the third inspection station..	76
Table 7: Confusion matrix of all samples that categorized as either good or NG.....	77

LIST OF ABBREVIATIONS

BLOB	Binary Large Object
CCD	Charged Coupled Device
CMOS	Complementary Metal Oxide Semiconductor
FIS	Face Inspection Station
FPGA	Field Programmable Gate Array
GAF	Gaussian Adaptive Filter
GUI	Graphical User Interface
ISO	International Organization for Standardization
KLD	Kullback-Leibler Distance
NDT	Non-Destructive Techniques
ODIS	Outer Diameter Inspection Station
OOP	Object-Oriented Programming
P2C	Polar to Cartesian
PDF	Probability Density Function
PLC	Programmable Logic Controller
ppm	Parts Per Million
ROI	Region of Interest
RPM	Revolutions Per Minute
RSIS	Rubber Seal Inspection Speed
SDK	Software Development Kit
STD	Standard Deviation
VisiBear	Machine Vision Based Bearing Defect Detection System

CHAPTER 1

INTRODUCTION

1.1. General Context

Nowadays, customer satisfaction is the key to survival of the companies. That is why the companies around the world find themselves in a competition. The most important determinant of gaining customer satisfaction is the quality of the products. Ensuring the quality of the products has always been an obligation to satisfy the customer. For this reason, many manufacturers are trying to do quality control from the customer's point of view in order to increase the quality of the product produced. With the impact of the recently developing technology and globalization, customers have more careful over the products they buy for use. Even if the product functionality is expected, the appearance is another important demand for customer [1]. By this reason, the competition between the manufacturers is based on the extra functional features they add to their products or to send the product to the customer completely without any defects. At this point, it must be to perform visual inspection on every product produced in order to ensure that it does not have any visual defects.

It is one of the most basic control applications to make quality control visually on the products which are produced in all sectors and all over the world before they are sent to the customer. Since it is one of the final control procedures, it is carried out at the end of the production lines. It is also critical and important because it is the last step in which a product with a visual defect can be stopped before it is sent to the customer. Visual quality control is applied in most sectors by visual quality control workers whose main job is to examine the products produced. However, given the increased consumption and the amount of product produced, it is a great risk to expect the efficiency of this manual operation to be sustainable and the reliability of the audit.

Visual inspection performed by visual quality control workers has great advantages when considering the geometrical and characteristic variations in the products, however the human factor brings many disadvantages. These disadvantages can be listed as below.

First of all, it can be said that there is not always the same attention and motivation during the working period. The most important reasons of this situation can be listed as fatigue or demoralization.

In addition, the variability in the decisions of different workers on the same product appears to be a disadvantage. Moreover, it can be said that the wrong decisions made on similar mistakes have repeatability or that the decisions made when the same product is shown to him again at different times are inconsistent. As mentioned above, these disadvantages and uncertainties are the factors that directly affect decision sensitivity and accuracy. In order to overcome this situation, machine vision systems are proved to be the most suitable system by many applications.

In machine vision and decision making systems, all the disadvantages, variables and uncertainties will be eliminated. By this way the same decision will always be taken on the same product.

1.2. Main Objectives

A Machine Vision Based Bearing Defect Detection System (VisiBear) system consists of two main subsystems. First, the hardware-based subsystem to obtain the product image to be examined. It has the task of receiving the optical image by the processing platform and converting it into digital data. The second is a software-based image processing subsystem. It consists of pre-processing of achieved digital data, obtaining feature vectors and image processing methods developed for final inspection results.

The first aim of this study is to design the product to which image acquisition subsystem will be applied according to mass production conditions. First and foremost, any VisiBear system should be faster than production speed, cost effective and highly accurate. However, in order to combine an efficient VisiBear system, audit requirements must be tailored to the product to be examined. Furthermore, it is absolutely important that the system shall be design according to the manufacturer's specific requirements. Therefore, it is important at the outset to identify both the problem and the manufacturer-specific product characteristics in a completely clear.

The second objective is to develop fault detection method for bearing-specific surface control. The method also should be developed suitable for surface inspection of various bearing. In addition, when mass production conditions are taken into consideration, it is very important to control the false alarm rate, to prevent unnecessary stops in production and provide the defect detection at maximum accuracy.

The second objective is to develop fault detection method for bearing-specific surface control. The method also should be developed suitable for surface inspection of various bearing. In addition, when mass production conditions are taken into consideration, it is very important to control the false alarm rate, to prevent unnecessary stops in production and provide the defect detection at maximum accuracy.

1.3. Organization of This Thesis

In section 2, the definition and application areas of the bearings will be mentioned. Then the production process of the bearing will be explained briefly. Following this, general information about quality control will be given and visual defects specific to bearings will be identified. In the present case, how visual quality control is performed, advantages and disadvantages will be mentioned. In this thesis, it will be explained how to overcome the disadvantages.

In section 3, a detailed description of the equipment of the system to be developed in order to prevent the sending of visual defects to the customer will be explained. In addition, the complete installation and capability of the developed machine vision based bearing defect detection system will be explained.

In section 4, all image processing methods used to detect visual defects will be described in detail. First, after obtaining the bearing image, the process of detecting and separating the bearing from the background, cutting and resizing the image separated from the background according to the specified boundary coordinates will be explained. Next, data preparation will be performed by identifying the regions with Circular Hough Transform (CHT), transforming them into Cartesian coordinates by P2C and dividing them into regions to be examined by segmentation. Then, the methods applied specific to the defects will be explained.

In chapter 5, the results of all detection algorithms will be given. In addition to these results, system reliability will be demonstrated with confusion matrices which will show system accuracy.

Finally, in chapter 6, with the conclusion and future works, all thesis will be evaluated and future studies will be mentioned.

CHAPTER 2

QUALITY CONTROL

2.1. Bearing Industry

Bearing is a machine element which allows the parts rotating in different directions with respect to each other to perform this movement with minimum friction and to reach higher speeds by using less power. Bearings, which are mainly formed by the combination of 4 different main parts, are used for bearing shafts which can be produced in different sizes for bearings and shafts of different sizes. Since bearings are precision machine elements, their production requires high technology and meticulousness. What makes the bearings important is the transmission of the required movement with the least possible friction, i.e. with minimal compromise of power.

Nowadays, with the development of machine technology, the usage areas and ratios of the bearings used for bearing of moving shafts to fixed bodies are increasing more. This machine element, which is indispensable in machine design, has many varieties. They can be produced using the most modern manufacturing methods and high quality materials. Among the many bearings, it is important to choose the right bearing in terms of variety and size for optimum machine design.

All bearings have different characteristics, but there are many similar aspects. Therefore, it is not easy to choose the most appropriate bearing, but the main purpose of bearing selection is to ensure that the bearing is long-lasting and fully functional. In addition to the bearing's dimension, the type and quantity of the bearing load, the expected service life and the bearing safety are taken into account when selecting the bearings.

2.1.1. Bearing Manufacturing Process

The first process in bearing manufacturing is hot forging and cutting. They are forged or cut according to the type of bearing to be manufactured.

Hot forging operation, rod-shaped steel materials are heated in induction furnaces up to 1200 ° C and the inner ring and outer ring parts are obtained for the other operation by applying the appropriate force according to the ring diameters in the hot forging press. These parts are also obtained from the cutting operation. Inner and outer rings of bearings are obtained from cutting process according to suitable widths and diameters in cutting machines.

In the subsequent process, the forged rings are subjected to spherical annealing to ensure that the structure is homogeneous and the rigidity is suitable for the turning process.

Cut and forged and annealed rings are subjected to cold roll forming that they are shaped. During this operation, the material structure is deformed in a controlled manner. Cold roll formed rings are shaped on CNC lathes or single turning machine that are arranged for successive operations. The structure and hardness of the material is made suitable by heat treatment of the turned rings. Grinding and superfinishing processes of the ring, outer diameter, bore and raceways are ensured by grinding operations.

Bearing components are cages; steel, brass and plastic materials. Bearing seals are produced from sheet material or rubber material and are installed with press machines in automatic lines.

The assembly process of the bearings can be carried out in automatic lines according to the types and customer demands without touching the hand and 100% controlled or manually. After the inner and outer rings are matched and the balls are placed in the raceway, the cage is assembled, the bearing is washed completely and the grease is injected into the bearing and the seals are installed. The final product

appearance with all the components of the bearing is shown in Figure 1.

The final checks of the bearings on the lines, in particular the noise levels, are 100% checked. With the conservation applied at the last station of the lines, the bearings can be reached / protected before they reach the end user or during the shelf life without being affected by environmental conditions. The final stage of production is the packaging process. The packaging process is made according to customer specifications and product specifications of the bearings manufactured for different sizes and different usage areas and shipped to the customers.



Figure 1: Bearing components.

2.2. Quality Control

The perception of quality control is changing day by day. Even the definition of quality term has been tried to be made more comprehensive by constantly discussing and changing it over time. The most recent definition of the International Organization for Standardization (ISO) is the degree to which an object's unique characteristics fulfill the requirements [2].

The assurance that the products produced can be sent to the customer 100% defect-free has been a necessity to satisfy the customers. At the beginning of industrialization, the people who developed the product were also responsible for its quality. However, parallel to the global increase in production requirements, production practices and techniques have gradually increased. With the understanding that the relationship between the customer and the manufacturer is not only customer-oriented, it has also led to the development of a quality perspective. In fact, many other parties of interest should be taken into account, as they are or are affected by the quality of the product [3]. These parties include employees, suppliers, investors and so on, and it includes others.

With the increasing importance given to quality, the quality control process has become a continuous process starting from the production of the product and applied throughout the entire process. Instead of the whole process control, this study focused on the quality control task of the product made just before it was sent to the customer.

As in all industrial sectors, the quality control performed before the product is sent to the customer can be grouped in two groups.

- Technical control: This stage can be said as the step in which all technical details regarding the operation of the produced product are checked. These are the defects that can occur in all production processes. Dimensional tolerance differences, internal structure defects, etc. Examples can be given.
- Appearance control: In this type of control, it can be said to examine the defects that do not constitute any obstacle to the proper operation of the product produced. These are purely visual defects and can be exemplified as scratches, impact, rust etc. formed on the outer appearance of the product. Such visual defects may occur during the manufacturing process, transportation or even during the use of the product. As a customer, including all sectors of the world, no one wants a visual on the product.

2.2.1. Quality Control for Bearings

In order to have a say in the market share in bearing production, it has become essential to be ahead of its competitors in quality control techniques. In this respect, it can be said that this is the first prevention study that needs to be done to examine the causes of defects and to improve the associated process steps by going back as far as possible. As a result, the visual defects that may occur due to production have been reduced to a certain extent. However, ensuring that the product with a visual defect is reduced in production cannot be guaranteed to reduce the visual defective products that can be sent unintentionally to the customer. It should not be forgotten that customers also perform their own visual inspections on the products they buy.

Technical faults in bearing production can be measured by comparing them with the reference gauges that have been produced before and are assured of all technical information. Technical s can be exemplified as geometric dimensional or mechanical bearing faults. These faults are usually caused by malfunctions or incorrect adjustments of the machine tools. Defects due to such undesirable conditions directly affect the whole production.

There are many different methods for controlling dimensional and geometric defects, inner-outer ring diameter measurements, hole diameter measurements, surface roughness and thickness are actively used in the bearings. Some of these methods are performed on certain samples outside of serial production using appropriate calipers and micrometers. In addition, in many production processes, measurements are taken at the time of production and both the efficiency of the production is recognized and the integrity is ensured. These techniques are sometimes based on image and signal processing or mechanical methods, and include electronic and pneumatic indicators, optical and imaging senses, and so on. It includes many technologies such as [4].

In case of visual defects, the quality control to be applied becomes more complex. These defects can generally occur during production processes or occur

randomly during product use. Since the occurrence of defects on the products may vary from piece to piece, all products must be subject to checking. Especially when today's production units are taken into consideration, it is necessary to realize the control process very quickly. Furthermore, in mass production conditions, only non-destructive control techniques can be applied, since the product to be inspected will be used in subsequent production stages. When it comes to using only non-destructive testing techniques for defect detection, it is a major drawback that there is no standard in the bearing industry for the detection of visual defects, that is, the lack of information on the shape or size of the visual being detected. In particular, the examinations carried out on the bearings to date have been largely carried out by people.

2.2.2. Bearing Surface Inspection

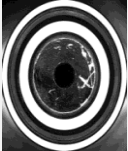
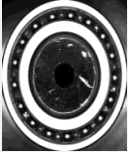
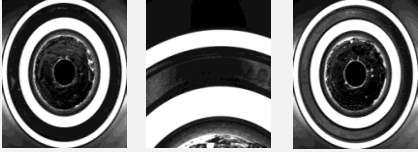

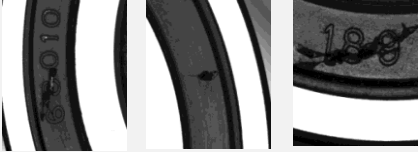
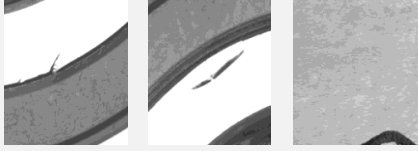



In all production sectors, quality control is carried out at the end of production lines as the last step of production. The reason for being an important procedure is that it is both the last step of the audit and the last stage of detection if a defective product is produced before it is sent to the customer. In the manufacture of bearings, especially in bearing bearings, the surface appearance (any deformation) after the seal have been installed greatly influences customer perception. In addition, it is of great importance in ensuring that the grease inside is sealed during operation. For this reason, it is necessary to carry out quality control on both the seal regions and the metal regions before they are sent to the customer.

2.2.2.1. Surface Defects

Any deviation from the product that is standard or normal in the product specifications is called abnormality. On the other hand, if this abnormality exceeds the acceptance limits set by the customer, this is called a defect. As in all industrial sectors, the main factor that determines the product quality is the consistency of the single type production for each product. All types of bearing production can be more than about 300,000 units per day. Each of the different types produced is trying to ensure this consistency within themselves in terms of quality. However, this consistency cannot be achieved as almost every industry. Visual defects can affect the

entire bearing surface or occur locally. These types are shown in Table 1.

Table 1: List of the main potential defects with their characteristics.

TYPE	Cause	Acceptance Limits	Frequency (PPM)	Examples
Reversely Assembled	Seal assembly process	Area = Whole area	~ 200	
Missing Rubber Seal	Seal assembly process	Area = Whole area	~150	
Deformation	Seal assembly process	Area ≤ Whole area	~400	
Overlap	Seal assembly process	Lenght ≤ 1.5 mm	~100	
Scratch on Rubber Seal	Seal assembly process	Lenght ≤ 1 mm	~250	
Scratch on Metal	Product handling	Lenght ≤ 1.5 mm width ≤ 1.5µm	~450	
Impact	Product handling	Lenght ≤ 1.5 mm width ≤ 1.5µm	~350	
Rust	Insufficient conservation	area ≤ 0.2 mm²	~600	
Shoe Trail	Production process	Lenght ≤ 1 mm	150	

- Local appearance defects: If there is a local disruption on a surface other than the reference tissue, this is defined as local defect. It represents only the differences that occur in a particular area of the surface to be inspected. These types of defects appear on the bearing surface and are often the most common types of defects.

These defects, scratches, signs, geometric deformation, dust and so on, and may be of different shapes and sizes. However, they can all be classified into two general types of defects. The first is on the surface, the second is the defects on the surface, but having a depth.

Table 1 shows the common visual defects that may occur on the bearing surface. It includes visual defects for all different types of defects, which are usually created based on customer criteria and audit experience. This information includes the type of, dimensional tolerance ranges (mm), and frequency of occurrence (ppm).

- Global appearance defects: Global defects are created to affect and cover the entire surface of the bearing. Such defects usually occur in the end face or outer diameter areas of the bearing during the grinding process. This process is carried out in order to include bearing dimensional boundary conditions within the desired tolerance ranges and to smooth the surface. During the process, visual defects covering the whole surface occur due to any problems such as rotation speed and feed rate of the stone that may occur on the processing table.

In fact, the visual defects on the bearing surfaces (provided that they are not too large) have no effect on the operation of the bearing. This is all about the aesthetics of the product, which will be delivered to the customer. However, it should be borne in mind that rusts are very important because they both affect the working principle of the bearing and can be directly noticed by the customer. The main reason for affecting the working principle is that rust that may occur on the metal surface can progress during the overseas shipment to the customer or during the operation. For these reasons, it is critical that even the smallest rust defects can be detected.

2.2.2.2. Current Setup: Manual Visual Inspection

At the end of the bearing production lines, visual defects on the surfaces of the bearings are realized by the visual quality control workers under bright light. The task of these workers is to examine each product produced completely and to prevent the defective product from being sent to the customer. Although these workers work according to the 8-hour shift system, they are forced to control thousands of bearings during their duty due to the high production volume. These defects will be listed as a list according to their severity. In order to make these lists more descriptive, photographic images specific to visual defects are used. Acceptance tolerances of certain types of defects may vary from bearing to bearing. Furthermore, more importantly, different customers may have acceptance tolerances that must be respected. Together, all these factors complicate the process that quality control workers have to do.

As already mentioned, the greatest advantage of human monitoring on bearing surfaces is the flexibility shown in finding visual defects that have a great deal of variety in size and shape. However, in addition to this important advantage, there may be situations (human motivation, fatigue, material or moral distress) that, by nature, can directly and adversely affect decisions made during the working period. In addition to such negative situations, it is the reproducibility of the decision made by the same auditor during the inspection of the same product [5, 6]. Such disadvantages bring uncertainties and lack of sensitivity. In addition to all these factors, the visual inspection of the product may differ from visual inspection workers. Finally, said visual defects may be very small and in such cases may escape the control of the human eye due to the large number of products.

In order to overcome all the disadvantages described, machine vision-based automated systems have proved to be one of the best methods of confidence in industrial production [7]. Decision variability, motivation and subjectivity among quality control workers are eliminated in these systems. That is, no matter how much inspection the product undergoes through these systems; the result will not change. In addition, it is possible to detect visual defects with high sensitivity and accuracy as

well as high resolution, and this detection can always be done at the same performance level.

2.3. Non-Destructive Testing for Surface Inspection

The objective of Non-destructive testing (NDT) is subsequently to distinguish any defects that will influence the accessibility, security of use [8,9]. These methods play a vital part within the quality control process, not only the quality of the final item, but also the quality of the gathering parts as well as the starting raw materials.

Since the starting of the 20th century, the improvement and application of NDT techniques totally different industrial segments have been developing quickly. It has presently ended up an fundamental portion of each industry at all stages of the production process. New procedures are being routinely presented to reply to different industrial issues in different segments, including nuclear, aerospace, civil engineering and automotive industries.

Within the writing, NDT methods are as a rule classified into two families agreeing to whether they favor the detection of surface defects or internal defects [10]. Typically the foremost vital calculate to regard when choosing the suitable strategy to perform the intended inspection task. In any case, this choice intensely depends on other critical criteria as well. A few of them are physical imperatives such as the nature of the reviewed parts (material, shape, etc.) and the environment in which the review is to require put (thermal, chemical, pressure, radioactivity, etc.). And other related to the taken a toll of the proposed strategy (material, labor, time devouring, etc.).

In any case, it is critical to audit other NDT methods to explore their ability to perform superior within the case study presented in this work. We'll display the foremost widely utilized strategies in this category. A few of these criteria are forced by the particular characteristics of bearing surface review, whereas others are characterized by the industry.

- Inspection tasks: What is the inspection process looking for? In our case the detection of surface defects is the main aim.
- Ease of automation: The automation of the control procedure is essential to improve the reliability of the control. Therefore, an important requirement for the audit system is the automation of the entire procedure.
- Product handling: Products that reach this inspection stage are finished products that will be delivered to customers, so they must be used appropriately during the inspection. Preferably, a non-contact NDT technique will be used to avoid any modification of the product.
- Record keeping: The most reason of the review method is to minimize the client returns for flawed items. When a client returns with a complaint around a inadequate item that he received, the industry must be able to appropriately react to his complaint and to confirm the cause of this mistake. As a result, it is fundamental to keep a record for all the products that have been assessed and conveyed to clients.
- Industrial requirements: From an industrial point of see, numerous other angles of the assessment system have to be be taken in thought, basically the taken a toll of assessment and the natural affect.

CHAPTER 3

MACHINE VISION BASED BEARING DEFECT DETECTION SYSTEM

The overall physical configuration of VisiBear systems are used for inspection of fruits and vegetables as well as for the inspection of steel surface in the steel industry [11, 12]. The lighting unit is used to distinguish the object of interest. In order to obtain a digital image of the product illuminated by light, digital cameras are used. The camera alone is insufficient to obtain the image because the image must be focused and dropped to the camera's sensor. At this stage, the lenses are used together with the cameras. After the digital raw image is obtained process continue with on the FPGA (Field Programmable Gate Arrays) cards. And then the general processing systems controls the VisiBear system. With using image processing techniques on these two platforms, the final decision is made for the examined product.

VisiBear systems generally consist of two main subsystems. The first is hardware-based and the second is a software-based subsystem. As in many other applications hardware-based system converts the optical scene into digital data. In this work FPGA card is used to transfer the raw image to the main system. At the same time FPGA card applies some morphological operations. After these processes it transfers the processed image to the main processing system.

Generally, these systems consist of lighting system, camera, lens and processing platforms. In some industrial applications, the number of these components may be increase. The software-based image processing subsystem contains the analyzing methods. At this system obtained images are analyzed and the feature vectors are extracted for making final decision. As applied in this thesis, integrated systems can be used both to control the hardware components within the VisiBear system and to use multiple software solutions that can manage the whole

system in software.

One of our first goals is to understand the requirements of the bearing industry in order to determine the VisiBear system requirements to be established and to make the system suitable for these requirements. By this way it is possible to select the necessary equipment such as cameras, lenses, lighting systems and software platform for the VisiBear system by following the specified requirements. Finally, after the necessary hardware adjustments are made on the prototype system the software works can be started.

3.1. Inspection Requirements and Conditions

First of all, when designing the VisiBear system, it should be ensured that this system is fast, reliable and cost effective. However, while paying attention to these requirements, sensitivity conditions need to be determined in more detail in order to design an efficient VisiBear system. In other words, it is very important that the application is designed to be specific. Therefore, it is essential to determine and carry out the design process together with the manufacturer.

- Bearing's seal surface complexity: There are both flat and cylindrical surfaces in the inspection areas of the bearing. In addition, the bearing type 6806 is manufactured with a rubber seal, which has irregularities in different parts of the rubber seal. These irregularities arise from the embossed mark on the seal and the seal's lips necessary for mounting the seal to the inner / outer grooves. Embossed mark is the first and most compelling part of the irregularities; it has a structure that protrudes from the normal surface of the seal, thus leaving details that can be detected as defects in corner detection algorithms and therefore when converted to a binary image. Under no circumstances should these details be identified as defects and captured by VisiBear. However, in some cases, the actual flaws may coincide with these embossed marks. It is critical to catch the defect and not to send it to the customer. Secondly, the seal's lips, which are fixed to the bearing, are design deeper than the normal surface of the

seal. Because of this height difference, illumination level is different, so the seal surface and lips are examined differently as ROI for inspection.

- Variability in defect types: The bearing has a wide variety of defect types on both the metal surface and the rubber seal. Defects of this variety are generally examined for the size, shape and possible cause of the defect. Some of these defects can be defined as scratches, bumps, rust. In addition, these variations can cause new defects to occur with changes in production processes. The developed VisiBear defect detection system should be able to detect all defects irrespective of the type of defect. The most important type of defect in the designed system is the formation of rust on the metal and the detection of the smallest rust defect is essential. Indirectly, the resolution of the selected camera should be high enough to detect the smallest rust defects.

3.2. Camera Selection

The first step in VisiBear system design is to identify the appropriate camera. First, it is necessary to consider the size and shape of the product to be examined. However, there is also a much more important issue, which is the level of detail of the defects to be inspected. The determination of system requirements described in Section 2.2.2.1 will also be effective in camera selection. It is one of the key points to determine these requirements as accurately as possible so that the camera to be selected is sufficient for the requirements.

The cameras used in quality control systems and image processing applications have far superior features than normal cameras. In addition to their superior features, they are designed to be compact and small so that they can be used in all applications as far as possible. In addition to all these features, they are manufactured to have a durable structure for use in harsh industrial environments. For these reasons, such cameras are called industrial cameras. In fact, one of the biggest benefits of industrial cameras is that the images obtained are generated as raw data without compression and no processing. In all image processing

applications, no data loss is desired in the images.

Recently, in addition to industrial cameras, smart cameras have become increasingly popular. Smart cameras have a hardware processing platform that can run both camera and image processing software on their bodies. In other words, besides image acquisition, image processing can also be done by itself. Although it seems to be very advantageous compared to industrial cameras, they are used in special applications and inadequate in general applications [13]. In short, it is limited in capability because it cannot be updated or added software, and is therefore not preferred in VisiBear systems.

3.2.1. Area Scan or Line Scan

In the selection of cameras that can be used in machine vision systems the alternatives are almost close to infinity. One of the most critical points in VisiBear system design is to decide on the camera scan technique. Scan techniques are divided into two groups as line scan and area scan. Although the aim is the same in both technologies, they are very different in terms of image capture logic. The choice of camera with scan type is all about the specific application.

An image consists of a certain number of lines. Line scan cameras use only a sensor of 1, 2, or 3 lines of pixels. When the object passes the camera or when the camera moves over the controlled object, the image data is captured line by line, then separate lines are recreated into the entire image during the processing phase. Since line scanning systems require moving parts to create the image, they are well suited for products in continuous moving or high speed applications. One of the best examples is the systems used to detect fabric defects. It is seen that line scanning cameras are used in the majority of such applications [14]. In addition, this type of practice is very common in the literature [15 18]. On the other hand, the disadvantages of field scanning cameras in such applications are mentioned [18]. Although line scanning cameras are used in moving fabric applications, there are applications in which field scanning cameras are used in stationary fabric inspections.

Briefly, lines are taken from the fabric surfaces passing at high speeds by line scanning cameras. To achieve the images, it must be synchronized with the direction of movement of the product line. It is important to remember that the triggering process for synchronizing with line scan cameras can be complicated to ensure a smooth image. In addition to fabric applications, line scanning belts are used too in similar applications such as conveyor belt inspections [19 21] and steel surface inspections [22]. In all of these applications, the cameras are fixed and adapted to move under the object is examined. There may also be applications in which the object is stationary and the camera is moved. However, they all have one thing in common: the surface of the object to be examined is too large, so the area cannot be captured with the scanning camera at one time.

In contrast, field cameras have a sensor having a plurality of pixels in both dimensions, either rectangular or square. The capturing mechanism of the image is divided into two as global shutter and rolling shutter. Generally, the global shutter is used, because the image data is taken instantaneously and all in one step. In addition, it is suitable for applications where the product to be imaged is stationary or moves very slowly. At the same time, they are used to capture the image of the entire relevant area of each product separately. As with line scan cameras, it is possible to capture continuous images of the products to be inspected in the area scan cameras but it is necessary to crop each image and combine them in the correct order. This is also possible with an extra software. Line scan cameras have advantages in some applications. Instead of using multiple area scanning cameras on very large surfaces, this surface can only be made with 1-line scanning camera. By rotating or moving the relevant product in front of the line scan camera, the image of the entire surface can be obtained.

It is suitable for very special applications such as being able to display the bottom of the part in conveyors, i.e., for unobstructed visualization in confined spaces and this provides a great advantage. In addition, continuous images can be created with line scan cameras that can eliminate the limit of resolution. Images with a higher resolution can be obtained in some respects when compared to field scanning cameras. It should be clarified that the resolution of the line scan cameras is

limited to the horizontal axis, whereas the resolution in the vertical direction will be determined by the size of the part.

Despite these advantages, line scanning cameras also have many disadvantages and have been effective in deciding not to use them in our application. In this work the bearings are inspected one at a time and for all bearings each inspection must be completed before the next bearing arrives. In order to increase the inspection speed as much as possible, it would be more appropriate to obtain the image at one time. This eliminates the need for extra equipment to be used in the line scan camera. In addition, field scan cameras can focus on a specific scene much faster. They can be installed much faster and are generally cheaper.

Finally, system integration of line scan cameras can be difficult for system settings. It is necessary to synchronize the speed of the product and the exposure speed of the camera.

The difficulty is the unwanted changes in system speed. Therefore, an additional hardware, usually is called incremental encoder, is required to adjust the line speed to match the current speed of the material.

3.2.2. Monochrome or Color Camera

All digital camera sensors are made up of millions of pixels, which are the smallest units of the image. These pixels are making the image possible. Each pixel consists of light-sensitive tiny sensors are called photosites or cavity. When a mechanical or electronic exposure is activated on a camera or industrial cameras, the photons are falling on these sensors.

When the exposure is finished, each pixel is reactivated again and different amounts of photons falling on each photosite. They generated different electrical signals and their value is determined by their power. The signals are then converted to digital values with an accuracy determined by the bit depth. This process may explain the acquisition of a monochrome image. But it is not possible to distinguish

the color scale from the obtained photon values.

With the use of color illumination, monochrome camera's black and white images show color related features. However, this solution is limited to only one color. In addition to colored illumination, this effect can also be created by a filter that can be attached to the front of the lens.

To create accurate color images, it is only possible with filters that allow the passage of certain light colors and will be placed on each photosite. Most existing digital cameras can only receive one of the three primary colors on each cavity, ie approximately two-thirds of the incoming light is discarded. As a result, the camera must bring the other primary colors closer so that each pixel can have all color values. The most commonly used filter, which contains the primary colors red, green and blue, is the "Bayer Filter". The human eye is much more sensitive to green light, so the resulting image uses two times more green filters in this filter so that it can be converged closest to it. The array only transmits the intensity of one of the three colors to each cavity to the sensor. Thus, each pixel represents the information of a single color. This is called RAW information. To create the final color image, the remaining two colors in each pixel are estimated (interpolated) using the eight surrounding pixels. This technique is called Bayer demosaicing or Bayer RGB conversion and is usually performed on the camera itself. This is the process of converting the Bayer primary color sequence to a final image with full color information on each pixel.

Unlike color, monochrome sensors do not use demosaicing to produce the final image; the values recorded on each photosite are effectively converted to the value in each pixel. This means that monochrome sensors can achieve a higher resolution than color sensors. However, in addition to the high resolution of the monochrome sensor, the flexibility of a color sensor should also be assessed and decided whichever outweighs. A camera with a color sensor can then always make it monochrome. Moreover, with color capture, any color filter can be applied post-production to customize monochrome transformation, whereas the effect of a lens-mounted color filter with monochrome capture cannot be reversed. it should be

selected if the camera is not a color-related application. Because the color filter in color cameras is naturally less sensitive. Bearings are manufactured with or without seal according to their application areas. Depending on the type of bearing to be used on the bearing seals, the assembly line may vary. However, certain types of bearings are produced on the production line where the VisiBear system to be developed will be integrated and does not vary between one product and the next. When integrated in different production lines and there is a change in the color of the seal, it can be customized only by changing the parametric values. As a result, the color has lost its importance for us, and monochrome cameras with high resolution have been used in order to detect defects more accurately and not to lose details. For the specific application presented in this study, monochrome images are essential.

3.2.3. Sensor Type

One of the most important steps is to decide to use the sensor manufacturing technologies such as charge coupled device (CCD) or complementary metal oxide semiconductor (CMOS). Both technologies do the work of converting photons into electrical signals. However, in both sensor technologies, the conversion methods and manufacturing methods are completely different from each other.

In addition to this technology, in CMOS sensors, a capacitor is placed on the sensor corresponding to each pixel. These capacitors are charged with photons falling on each pixel and converted into electric current. The voltage generated in the capacitor is proportional to the light intensity and exposure time. Unlike CCDs, electrons charged in capacitors by exposure to pixels are converted to a measurable voltage directly at the source through the independent electronic circuit of all pixels, rather than being transferred to a single output amplifier. The converted voltage can then be supplied to the analog signal processor.

In the case of CCD sensors, instead of applying individual conversion electronics to all pixels on the sensor, a transducer working for the single and the entire sensor surface is used to capture the captured light from the entire sensor surface. This technique leaves more room for pixels on the sensor surface, which

means that more light can be emitted in turn than CMOS sensors. Therefore, CCD sensors are more sensitive to light than CMOS sensors. On the other hand, CMOS sensors with independent converter per pixel mean that the converted voltage values can be read much faster than CCD sensors. That is to say, the CCD absorbers are prevented from blooming and staining caused by excessive light fall.

With the technological developments in recent years, modern CMOS image sensors have emerged as a powerful alternative to CCDs, although the trend in the sensor market is increasingly pointing to CMOS technology. In the literature, the advantages and disadvantages of both sensor technologies are reviewed [23]. The main advantages and disadvantages are mentioned [24, 25]. However, the main disadvantage of the CMOS sensor compared to the CCD sensor is the noise and poor image quality, especially in low lighting conditions. In order to overcome all the disadvantages of image quality in CMOS sensors, this sensor technology developing process is continuing.

Concluded that because of the low cost and power consumption of CMOS technology, integration capabilities, etc. It should be noted that CCD technology has a low noise level, so they have shown that there is no alternative for much more sensitive applications.

One of the important factors to be considered after deciding on sensor technology is the shutter type. The shutter prevents the camera sensor from being exposed to continuous light and only opens during exposure. The shutter speed adjusted according to different scenarios and the amount of light is actively involved in determining the correct amount of light that will fall into the sensor.

Dark images are displayed if the shutter speed is faster than normal, or brighter images than normal if it is slower. The shutter type is divided into global or rolling shutter. The difference is all about how light is dropped on the sensor. The global shutter opens the entire surface of the sensor simultaneously, allowing light to fall across the entire sensor surface. Although this type of shutter can be varied mechanically or electronically, electronic shutter is generally preferred in industrial

cameras. On the other hand, the rolling shutter creates the image by scanning the sensor surface, which does not open simultaneously, but allows the light to fall on the sensor at different times for each line, respectively. Generally, depending on the speed of moving objects or the selected shutter speed, it causes distortions during image formation and this type of shutter is unsuitable for many applications. This distortion is known as the rolling shutter effect.

For the bearing examination presented in this study, it was decided not to move the bearing to form end face images, but to obtain the images by turning the bearing during the acquisition of the images of the outer diameter. As a result, it is the right decision to use a global shutter to avoid future image distortion due to the slightest movement in the product.

3.2.4. Resolution

Despite all the steps described by camera selection, there are still many steps that can influence the correct selection. There are many options as a camera manufacturer in the world and they offer many options within themselves. Every manufacturer is trying to gain a place in the competitive environment by promising features such as improving image quality, faster and lossless data transfer. These features can be adjusted with software-based parameters such as ISO, gain, exposure time and gamma correction. However, it should be noted that improving the image with the software is limited by the hardware features of the camera, especially the pixel size and resolution. Therefore, the selection of the camera must first depend on its physical properties or characteristics, more precisely its resolution, pixel size and sensor size.

When selecting a camera, on the specification sheet, the sum of the number of pixels on the sensor is displayed as the resolution. This is not exactly accurate and sufficient to determine the required resolution. Thus, in industrial image processing, there may be another definition in which the resolution is indicated by how much of an area or the dimensions of the object being examined is indicated on a single pixel. To be more precise, the resolution detail is better than the smallest defect detail that

is intended to be found. As stated in the system requirements (section 3.1), the smallest defects to be detected have a size of about 1.5 μm in one direction.

In fact, there is no general rule that the smallest visual defect can be detected and associated with resolution in the image. However, how much information is required about the defect to be detected directly affects the resolution. As the number of pixels decreases, it becomes difficult to distinguish the defect from the normal surface. Providing the ability to classify defect detail as dimensional and formal is critical to assess its severity. In this study, the purpose of the audit system to be developed is to classify visual defects as well as detection.

3.2.5. Camera Interface

Finally, the choice of the appropriate camera is decided on the connection interface. The interface precisely establishes the connection between the camera and the data processing hardware and transfers the image data obtained from the camera to the data processing platform. Today, there are cameras produced with various connection interface technologies and it is best to choose the right interface according to the application. Here, the two most critical options to consider are maximum bandwidth and jumper length, depending on the data rate. In addition, the possibility of using a multi-camera system is another important factor.

Industrial camera production also has different options according to the connection interfaces. These connection interfaces have their own standards and can be named as IEEE1394, CoaXPress, GigE Vision, USB Vision and Camera Link [26]. In addition to these connection technologies, FireWire, Pixel-Shift and IP65 / 67 interfaces have been added. The USB and GigE Visions interfaces have been recognized as the primary choice in machine monitoring systems, as they do not require additional frame grabbers for operation, as well as ease of data transmission and addressing, as well as being cost-effective. For these reasons, only the two connection interfaces will be selected.

Developed according to the Ethernet communication standard (IEEE 802.3) protocol, the GigE Vision standard is the most commonly used interface in industrial machine vision systems. The main reason for this is that they can transmit 100MB / s data rate up to 100 meters without loss of data with a single cable without the need for any additional hardware. Besides, as mentioned earlier, it allows the creation of applications using multiple camera systems. This connection option has been decided since GigE Vision is the most suitable interface for multiple camera systems in the FPGA based cards.

3.3. Lens Selection

The term distortion is frequently applied alterably with decreased image quality. Distortion is an individual deviation that does not in fact diminish the information within the image; whereas most deviations actually blend information together to form image obscure, distortion essentially mislays data geometrically. This implies that distortion can really be calculated out of an image, while information from other deviations is basically disappear within the image and cannot effortlessly be reproduced. Note that in extraordinary high distortion situations, a few data and detail can be gone due to resolution alter with amplification or since of as well much data being swarmed onto a single pixel.

As with other deviations, distortion is decided by the optical plan of the lens. Lenses with a more extensive field of view will mostly display bigger distortion due to cubic field connection. Distortion is a third-order deviation, residual with the third power of field height for ordinary lenses; this means that wider sight (low magnification or short focal length) is more vulnerable to distortion than smaller sight (high magnification or long focal length). The extensive sight obtained with the short focal length lenses should be measured against any deviations (e.g. distortion) that occur in the system. Besides, telecentric lenses characteristically have very few distortions: a result of their function. The maximum resolution that can be achieved can be reduced when designing a lens with minimum distortion. To minimize distortion while protect high resolution, the complicity of the system must be enhanced by adding elements to the design or using more complex optical glasses.

Distortion is typically determined as a percentage of the field elevation. Typically, ± 2 to 3% distortion is ignored in a vision system if measurement algorithms are unused. In basic lenses, there are two fundamental types of distortion: positive, barrel distortion, where points in the sight become clear very near to the center; and negative pincushion distortion, where the points are so much far away.

While distortion in general runs negative or positive in a lens, it is not unavoidably linear in its needle over the image for a multi-element assembly. In addition, as wavelength amendments, so does the degree of distortion. At the end, distortion can convert with changes in working distance. Lastly, it is important to severally consider each lens that will be used for a significant application in order assurance the peak of accuracy when looking to disappear distortion from a system.

3.4. Lighting System

Certainly, a VisiBear system relies on quality images to verify quality control results. With high quality images, it enables the system to interpret the information that is targeted to be found from the object under examination in an accurate way, which increases the reliable and reproducible system performance. The importance of light is very critical as there is no image in all machine vision systems and even in all imaging systems when there is no light. Because, including the human eye, the light must be reflected on the object to be taken to form the image. Therefore, in all VisiBear systems, light is of vital importance with a direct impact on image quality.

Apart from the selection of cameras and lenses, which are more dependent on mathematical rules, as described previously, there are few known standards for the light system. There is a clear rule, however, that the well-designed and positioned lighting system should be able to minimize environmental influences (such as contrast) and highlight visual defects. In general, light system manufacturers offer their own catalogs to create the right lighting design for suitable applications. These catalogs contain lighting technical information to be followed in a practical way for their customers. In general, the geometric shape, size and surface properties of the object contain information on which many parameters are tested. As a result, the

prototype can be developed in order to obtain product images to be examined at the desired level depending on this information.

It is recommended to use a prototype design and technical information catalog with 129 different lighting options to select the appropriate lighting technique [27, 28]. Within this information, the appropriate light source to be used is determined.

3.4.1. Lighting Technique

Reducing glare and creating a stable lighting environment that is unaffected by outdoor lighting and ambient lighting changes can be shown as the purpose of lighting. However, the most important is to increase the contrast in order to better observe the desired properties. High contrast properties are of great importance as they facilitate the application of examination methods and increase the accuracy of the examination.

It is also very important for us that the light on the surface being examined is evenly distributed. It saves us from a few important situations such as the use of unnecessary algorithms and prolongation of the research process. It is necessary to provide the most suitable lighting for the designed system.

In general, a wide variety of lighting techniques are available. [28]. Depending on the surface of the object under investigation and the position of the object relative to the camera, we can classify these techniques into several classes.

- **Ring Lighting:** This type of lighting is mainly used to inspect object which has a normal or diffused surface. The object can be observed more clearly with light coming from different angles from all directions. Good image contrast can be achieved with adjustments in working distance and light distribution angle.

- **DOAL (CO - Axial) Lighting:** DOAL lighting technique provides the best contrast because it is uniform and diffused. Smooth surfaces appear bright and others appear dark because they absorb light. This type of illumination is used to inspect scratched or raised surfaces.
- **Dome Lighting:** Dome lighting provides a wide angle of illumination, although diffused. In this context, it is used for the examination of mat and non-flat or concave or convex surfaces.

3.4.2. Lighting Source

The main disadvantage of quartz-halogen lamps is their limited lifetime. The life span of this lighting source is around 2000 hours and is much shorter than that of fluorescent and LED lamps [29]. This means continuous maintenance changes will be made for VisiBear systems and hence increase costs. Another disadvantage is that they cannot provide stable light during the working period. This directly affects accuracy and sustainability in VisiBear systems. When the same bearing is passed under the inspection system for inspection several times, different decisions can be made due to the change in intensity and color of the light source. For these reasons, it was decided to abandon this light channel from the beginning.

In fluorescent lamps, a mixture of low pressure ionized gas mercury and inert gas is filled into the glass tube and electrode is present at both ends of this glass tube. When the electric current generated by the electrodes passes through the gas, the gas ionizes and emits light through ultraviolet radiation. To eliminate harmful ultraviolet radiation, these tubes are coated with various metallic and phosphorus salts, allowing only visible light to emit [30].

Although the initial cost of a fluorescent lamp is higher than that of a quartz-halogen lamp, lower energy consumption throughout its working life makes it less expensive. In addition, the lifetime is higher than quartz-halogen lamps, but is too short to compare with an LED lamp. They should be cyclicly changed every six months to give stable and healthy light. Furthermore, the light intensity known as

luminance is low intensity in fluorescent lamps and is inconsistent compared to LED and quartz halogen lamps. This is due to the unstable and unpredictable response of the gases used in the tube. As a result, fluorescent lamps cannot provide uniform illumination over the entire illuminated surface and therefore make inspection difficult.

Finally, it is necessary to look at the characteristics of LED, the most preferred light source in VisiBear applications. The LED is semiconductor and when activated, it generates light through the light emitting diodes. When an LED module is activated, electrons reunite with electron holes in the device to release energy in the form of photons [30]. LEDs are highly efficient, as well as being electrically safe because they operate at low electrical voltage and release a small amount of unwanted heat.

However, what makes LEDs so important for VisiBear systems is the light performance they provide. In addition to being able to deliver very bright light, the LEDs complete it with high light intensity and completely flicker-free. With these characteristics of LEDs, it provides a clean and noise-free way to inspect products or objects with high precision. In addition to enhancing audit performance and being reliable, they do not require much maintenance because they can last up to 100,000 hours. More importantly, the light outputs of the LED modules slowly drop over time, meaning they do not die instantly [31]. This helps ensure that the VisiBear system works well for a long time, avoiding a sudden failure that could result in a crash from the lighting system. The last important feature of LEDs is that they are physically separated and very small, so that they can be easily mounted on any platform. Thus, it is possible to produce light sources with different and complex designs. In addition, the LED modules are manufactured in square form, thereby creating narrow light that can direct light emission as desired.

For all these reasons, in this work, it was decided to use a diffused lighting system based on white LED modules. The lighting units to be used are then connected to the power supply via the driver circuit which controls the light output.

3.5. Processing Platform

The final step in VisiBear system design is the determination of the software processing platform. Nowadays, the manufacturers of these diversified platforms are in a fierce competition to develop the highest possible performance system. These platforms can be grouped under three main headings: multi-core CPU, GPU and FPGA [32].

Firstly, multi-core CPUs are produced by combining two to ten cores on the same integrated circuit to perform compute-intensive operations and accelerate it. Secondly, GPUs consist of hundreds of cores and are based on parallel processing logic to maximize efficiency. Finally, field programmable gate arrays (FPGAs) stand out a step when higher performance is required, especially in power calculation ratios.

Many researchers have sought to evaluate their performance in different sectors to compare these three platforms [3236]. However, the literature concludes that there is no definite winner in the face of different problems [36]. In fact, each of the aforementioned platforms has its own advantages, one step ahead of its application.

Modern GPUs are designed as programmable processors that consist of multiple processor cores. At first glance it may seem superior to CPUs in terms of the number of cores, but this is not always the case. Because GPUs do not do their own operations independently, they do this together with CPUs. Because GPUs are often used as computational processors with the main CPU, not as standalone systems. This is because GPUs are not designed to perform sequential operations. Similarly, GPUs are weak for non-parallel operations because they do not have the basic characteristics of branch prediction. In fact, GPUs are particularly suitable for addressing problems that can be expressed as data-parallel calculations in which the same program is executed in parallel by mapping to parallel processing threads on several data elements [35]. Although the GPU has its own high-speed memory, it needs to transfer data to the CPU memory as it is limited in space when large

amounts of data need to be processed. Because this transfer between the two platforms is slow, it causes undesired delays in the program and this is a major disadvantage for GPUs. Therefore, in order to make the most of a GPU's full performance, a trade between data transfer and processing parallelism must be respected. It should be examined according to each different situation without generalization.

On the other hand, FPGAs, configurable logic blocks, programmable input / output blocks present a completely different situation with their features including redirectable resource hierarchy arrays that allow these blocks to be connected to each other. Combinational and sequential circuits can be configured in FPGA logic design. This feature is the most important advantage of FPGAs over CPU and GPUs [35]. The function of the FPGA chips can be redesigned at the hardware level so that it can perform any desired operation according to the requirements of the developers. If a design is performed on the FPGA, the insertion must be reconfigured to meet the requirements. However, in FPGAs, re-synthesis and configuration are both difficult and time-consuming [37]. Therefore, in order to avoid these difficulties, Silicon Software has created a frame grabber card (microEnable IV-VQ4) with FPGA chipset and Visual Applets (VA) software to program these cards. This software uses model-based software language and the software design is created by combining the modular operators created. Each of the modular operators has been specially designed for a functional process in itself and has been created before the logic blocks that these operators will use on the hardware FPGA chipset. In addition, C ++ based Software Development Kit (SDK) libraries have been created in order to be compatible with software that runs on CPU and GPU and systems developed before FPGA technology. In this way, both the advantages of FPGA have been benefited and the difficulties it has brought with it have been avoided.

As a result, in our study, PC and FPGA were used together in order to create the control software much faster. Because the hybrid hardware option is the most flexible solution and the easiest to program while providing high performance.

3.6. System Design and Installation

This section describes the design and installation of the VisiBear system according to the visual inspection zones to be applied on the bearing. In fact, this stage was initiated immediately after the decision was made on the equipment to be placed on the machine to be used in mass production, see Figure 2. The reason for this is to determine all the requirements of the audit system to be established before implementation and then to design a system model that can meet these requirements. The VisiBear system, which is tailored to the requirements and will meet the requirements, is shown in Figure 3.



Figure 2: Visual inspection system “VisiBear”.

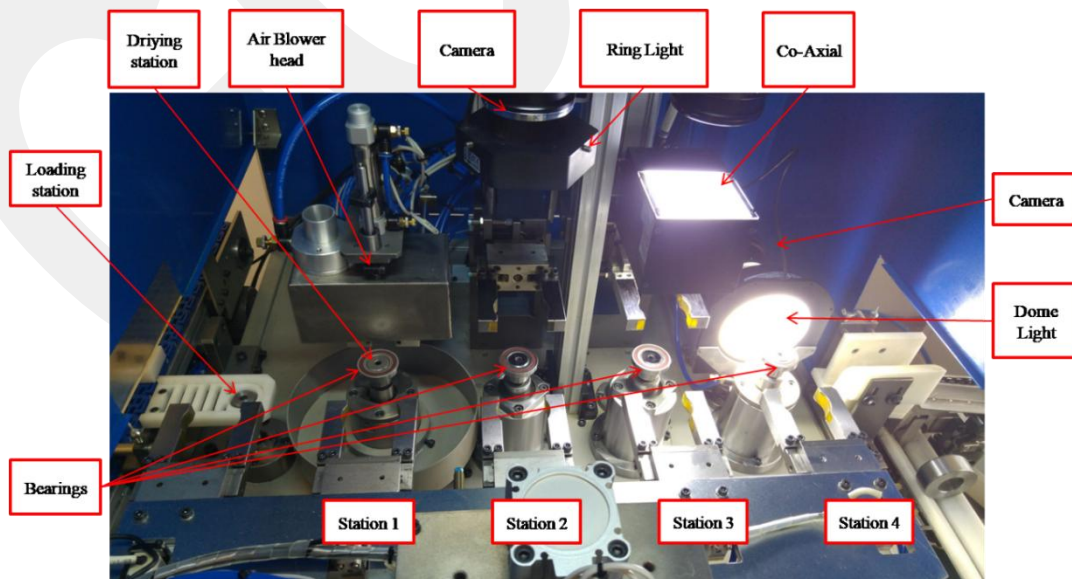


Figure 3: Physical system with visual inspection system

All the image processing hardware of the VisiBear system, which will be installed completely automatically and used in mass production lines, was decided just before the installation phase and the platforms where the image processing and control software operations would be run were determined. The camera, lens, lighting system and operating platforms, which are determined as a result of all the processes described and are composed of 4 basic elements of the imaging system, are shown in Table 2.

Table 2: Hardware specifications.

Camera	Area scan Monochrome camera CCD sensor with Global electronic shutter Resolution: 4896 (H) x 3264 (V) (16 MP) Sensor size: 26.93 mm x 17.95 mm type APS-H Pixel size: 5.5 μm \times 5.5 μm GigE interface
Lens	F- mount lens Fixed focal length: 46.5 mm Aperture: f/2.0 – f/22
Lighting system	Diffused lighting technique White LED modules Ring, Co-Axial, Dome iBluedrive controlled voltage output
Processing platform	PC FPGA: microEnable IV VQ4 - GigE/PoE Image processing: Visual Applets, C++/OpenCV

Since the fully automatic bearing machine is designed for visual inspection on both surface regions and outer diameter of the bearing, the visual quality control machine is designed to capture all of these surfaces and you can see this in Figure 3. Apart from all these, the surface of the bearings may remain liquid. This fluid can pass through conveyor belts which carry the task of transport during production or it occurs during the washing process (to prevent corrosion), which is one of the production processes. The presence of this fluid on the bearing surface can be perceived as a defect by the developed inspection software. Therefore, it is essential to get rid of the fluids just before the stations where visual quality control will be performed. All stations created with the design, except that the bearings are loaded on the inspection machine, are described below:

- Station 1 – Drying: This station is positioned just before the inspection stations in order to get rid of the previously mentioned fluids remaining on the surface of the bearings. The first technique that comes to mind for the bearing drying process is the centrifugal force which is also the simplest technique. The bearing is brought to the drying station by mechanical grippers and is seated on the piston of the station through the inner hole. After being seated, the bearing was rotated at 3000 rpm to dry under centrifugal force. However, since drying is a very critical process, it is essential to ensure that fluids are cleaned from the entire surface. Therefore, the air blowing head was added to this station as an alternative method. Thanks to this nozzle, the entire surface of the bearing is dried by blowing high pressure air with the centrifugal force.
- Station 2 – Defects inspection on rubber seal (RSIS): This station is designed to detect visual defects on rubber seals only. The light used for the detection of visual flaws was chosen in accordance with this surface, since the rubber seal were a surface that absorbs the light relative to the metal surfaces. Furthermore, the surface geometries of rubber seals are more complex than metal surfaces, so different approaches have been studied in the software developed for the detection of visual defects as well as the light source. The bearing is brought to the drying station by mechanical grippers and is seated on the piston of the station through the inner hole. The piston moves to the up position and the bearing is brought to the focus level of the camera. The bearing image is captured and all operations are performed to inspect the visual defects of the seal on the first surface of the bearing. After inspection, the first scenario, if there is a visual defect in the seal region of the first surface, the trigger signal containing the "NG" information is sent to the machine. This signal means that the machine will reject visually defective bearings from the mass production line. In the other scenario, if no visual defects are found on the first surface, the trigger signal containing the "OK" information is sent to the machine, which enables the machine to initiate automatic rotation operations for inspection on the seal of the second surface of the bearing.

When no visual defects are detected on both surfaces, the machine automatically transmits the bearing to the serial production line so that the next production process can be continued.

- Station 3 – Defects inspection on Inner/Outer Face (FIS): This station is designed to detect defects on the inner / outer rings of the bearing surface. The light source is chosen differently, because unlike rubber coatings, the surface to be examined is a metal surface and reflects light to a large extent. Briefly, the surfaces examined are completely different and all equipment except the light source is exactly the same, but the parameter settings change as described previously in section 3.4.1. In addition, the mechanical operating principles and software triggering scenarios referred to in station 2 of the machine are the same.
- Station 4 – Defect inspection on outer diameter surface (ODIS): Unlike the ones described in Stations 1 and 2, the outer surface of the bearing is not of a planar structure such as the sidewall surface. In other words, it is not possible to capture the entire surface at once for defect inspection. This station is designed so that the camera is fixed and the bearing is rotated so that the cylindrical bearing surfaces can be imaged precisely. As with other stations, the bearing is mounted on the piston of this station by means of a bearing gripper through its inner hole. After the machine starts to rotate the bearing with the predetermined Revolution Per Minute (RPM) using adjustable stepper motor with PLC software), trigger signal is sent to start acquisition processes by FPGA cards. Upon receipt of the trigger signal, the image of the entire surface is recorded in separate images with multiple exposures. Visual defect inspection is performed by finding ROI on these images. In addition, the software triggering and OK / NG separation scenarios are the same, although the mechanical operating principles specified at stations 1 and 2 of the machine are different.

In addition to the drying and visual inspection stations described as the main station, the remaining stations move the bearing from the first input to the last output without touching the bearing. These stations are designed as loading stations, transfer grippers, turning grippers and NG separators. Firstly, the loading station assumes the task of automatically loading the bearing produced on the serial production line into the VisiBear system. Secondly, transfer grippers perform the simultaneous transfer of bearings from one station to another within VisiBear. Thirdly, the turning grippers are located only on the second and third base stations and are responsible for rotating the other surface of the first inspected bearing to prepare the bearing for visual inspection. Finally, the NG separator station is located in VisiBear as the last station, and this station performs the rejection of the bearings that are visually defective from mass production. In addition, this station can collect the rejected bearings from the mass production into two different physical groups, face and outer diameter. In this way, it is possible to monitor on which station the defective bearing is detected. The entire management of the VisiBear system is controlled by the PLC.

3.7. Communication between PLC and FPGA

All mechanical controls on VisiBear are provided by the Programmable Logic Controller (PLC). As described in Section 3.6, the PLC manages all operations in VisiBear, such as loading the bearing, bringing all surfaces of the bearing to the relevant stations for visual inspection, fixing them to the camera focus position, and separating the defective bearings from mass production. However, all the image processing and the resulting decision are made by FPGA and C++. These two platforms must communicate between each other in order to operate synchronously. There is no "OK" or "NG" signal in these communication signals that only indicates whether the bearing is defective or not. In order for VisiBear to work smoothly and accurately, we can divide all communication signals into four groups, see Figure 4:

- **Trigger In: Check Trigger Signal** is the trigger signal generated by the PLC to be sent to the FPGA card when the bearing is fixed to the appropriate position on the machine to capture its image.

- **OK/NG Signal:** It is the trigger signal which is produced on FPGA board and sent to PLC system which contains information of whether the obtained bearing is visually defected by means of camera control software.
- **Complete Signal:** This signal is the trigger signal that is generated on FPGA board and sent to PLC system, which means that the camera control software has completed all operations. With this signal, the PLC continues to turn the 2nd surface of the bearing on the machine or to transmit it to the other station.
- **Run Signal:** It is the trigger signal produced on the FPGA board and sent to the PLC system. This signal contains information that the image processing software and hardware are active and running smoothly. Therefore, unlike other triggering signals, this signal is continuously sent to the PLC. If this signal is not sent to the PLC; The PLC will know that there is a problem in the image processing system for any reason, that no quality control is carried out on the bearing, and will stop the entire system and give an alarm.

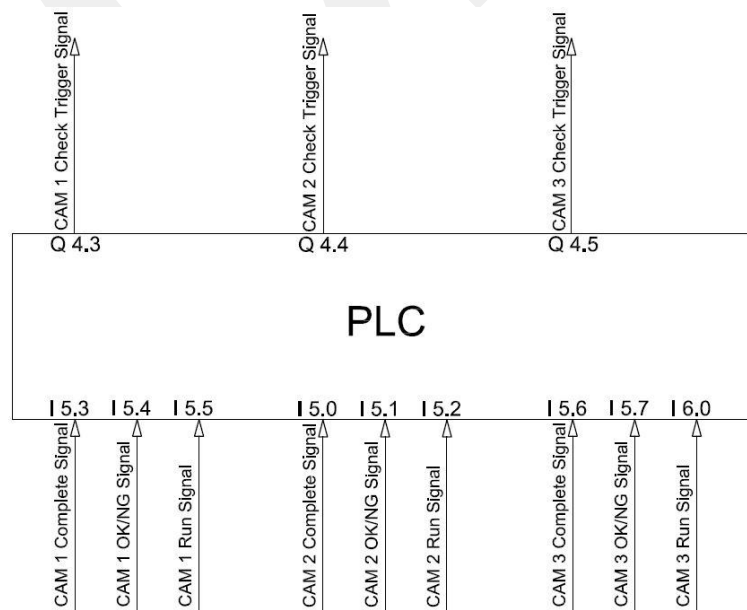


Figure 4: Trigger signals between FPGA and PLC.

Siemens S7-1200 is used as PLC and internal / external trigger signals which are accepted as standard among all PLC manufacturers are provided at 24 VDC level. The internal / external triggering signals of the FPGA board where visual quality control is performed are provided over 2.4-3.3 VDC level. In order for these two processing platforms to communicate healthily, the generated triggering signals must be converted into each other's voltage levels. In order to achieve these transformations, our original trigger cards were designed using the LM2596 Step Down Adjustable DC-DC converter, see Figure 5. The critical points in this design are both feedback inhibition and avoidance of delays in the trigger signals. Solid State Relay (SSR) is used to avoid delay in trigger signals. This prevents delays in the trigger signals caused by capacitors at the LM2596 inputs and outputs.

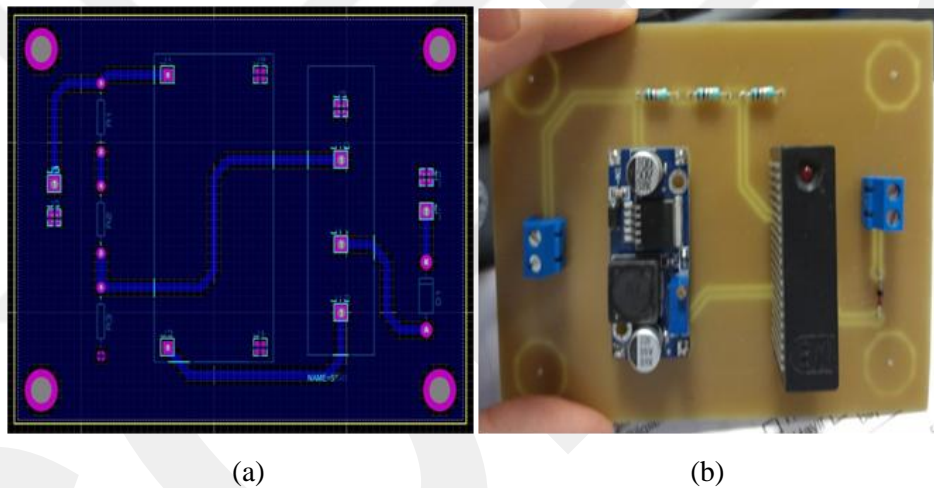


Figure 5: Design of trigger card, (a) PCB layout, (b) PCB.

CHAPTER 4

DEFECT DETECTION METHODS

In fact, it is generally preferred to use the camera settings and lighting settings instead of image processing methods to highlight defect contrast in VisiBear systems. However, it is inevitable to use image processing techniques when the variety of defects is very diverse. As a result, standard techniques such as point transformations, spatial transformations and morphological processes are used. The purpose of these techniques is to eliminate all the information except the defect, such as noise. The methods used are;

1. Thresholding grayscale image
2. Thresholding Otsu's method
3. Blob extraction
4. Resizing
5. ROI segmentation
6. Gaussian-Blur on grayscale image
7. Median filter
8. Thresholding separated regions with Otsu's method
9. Erosion/Dilation

and also the features are:

1. Mean
2. STD
3. Skewness
4. Kurtosis
5. Variance
6. KullbackLeibler Distance
7. Power Graphics
8. Shifting / Rolling window

4.1. Otsu Thresholding on Grayscale Image

First of all, the bearing is brought to the camera position and focal point by the machine. The coordinates of the bearing must be determined in order to be able to use them in the subsequent processes. For coordinate determination operations, 0-255 8 bit grayscale image must be converted to binary format. The most common method, Otsu's thresholding method, was used for this translation [39]. Since the light settings are fully adjusted to the region to be examined, no adaptive thresholding method is needed. Otsu's thresholding method:

$$\sigma_{\omega}^2(t) = \omega_0(t)\sigma_0^2(t) + \omega_1(t)\sigma_1^2(t) \quad (1.1)$$

Where ω_0 and ω_1 are the probabilities of the two classes which are determined by the threshold value t and σ_0^2 and σ_1^2 are the variances of these two classes. The threshold value T found by the Otsu's method minimizes this function.

4.2. Blob Extraction

The Binary Large Object (BLOB) extracting method can be defined as the process of converting only the information that is intended to be found on the binary image into representative information, whereby all the rest of the information is differentiated from the background. The first thing to do is to exclude all data except the object because there is no information with the product to be examined. The number of BLOBs is the sum of the white pixels that will enter the region. This number is used to determine the size of the BLOB so that smaller or larger BLOB information on the binary image can be filtered. Drawing the square / rectangular box, circle or convex body to be added over the boundary information is used to show the detected BLOB area [39, 40].

In our project, by examining all pixels for a BLOB, rectangle is drawn by finding four pixels with minimum X value, maximum X value, minimum Y value and maximum X value. The bounding box is pulled by taking the width given by $X_{max} - X_{min}$ and the height as $Y_{max} - Y_{min}$. The restriction box is also known as ROI, see Figure 6. The bounding box ratio of a BLOB is defined as the height divided by the width of the bounding box.

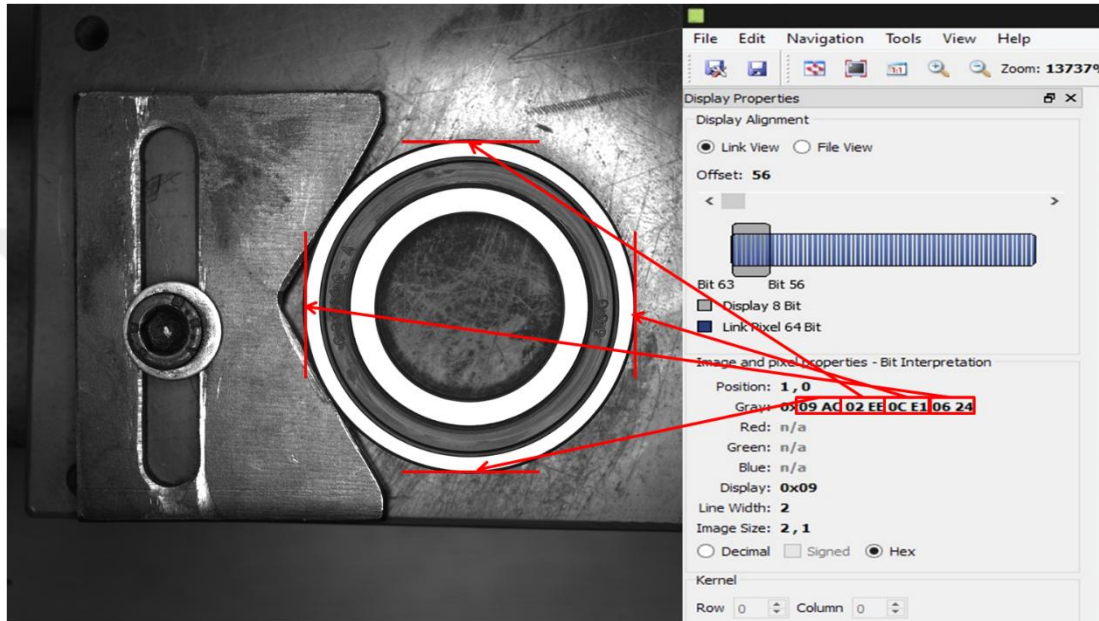


Figure 6: Detected bearing's outer ring boundaries coordinates.

As highlighted earlier, a BLOB consists of interconnected, i.e., groups of adjacent white pixels. Whether two pixels are connected, which pixels are adjacent, and which are not, are defined by the connection. The two most common types of connections are shown in Figure 7. 8 connections are more sensitive than 4 connections, but 4 connections are applied frequently because it requires less calculation, so it can process the image faster. However, as shown in Figure 7.2, the results of the two different connection options vary with each other. wherein the binary images comprise one or two BLOBs, depending on the connection.

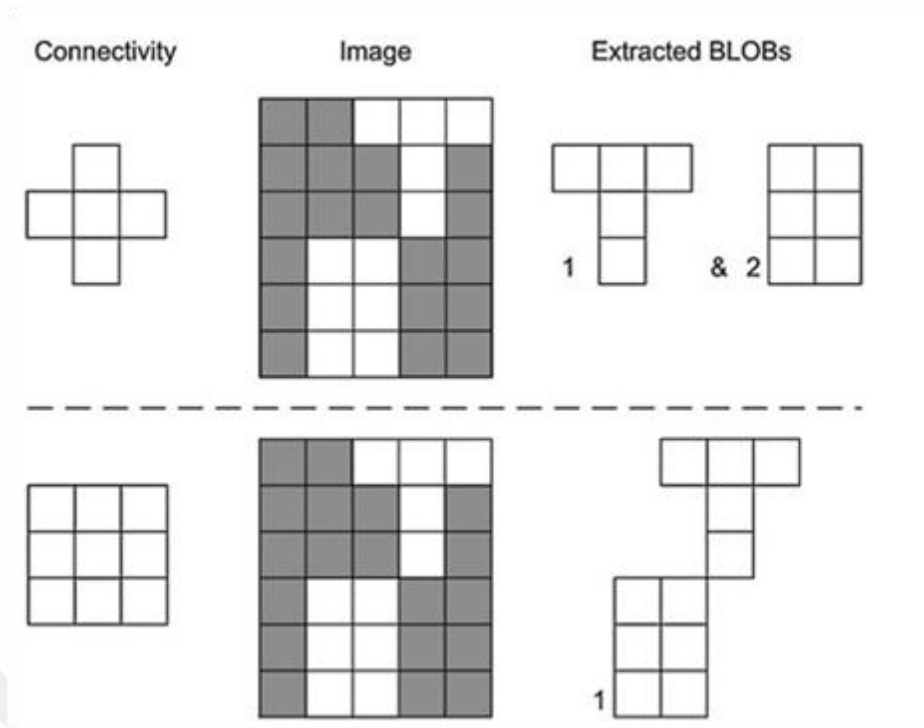


Figure 7: The effect of applying the 4 and 8 connectivity types.

4.3. Crop and Resizing

After the blob extracting process, the outer diameter coordinate information of the inner ring and outer rings of the bearing is obtained. From the coordinate information obtained, the image is cut by referring to the outer diameter coordinate information of the outer ring and only the new image is obtained on which the whole bearing will remain on the image, see Figure 8. This will allow us to reduce the image data we are going to work on and to enable the techniques to be applied much faster [41].



(a)



(b)

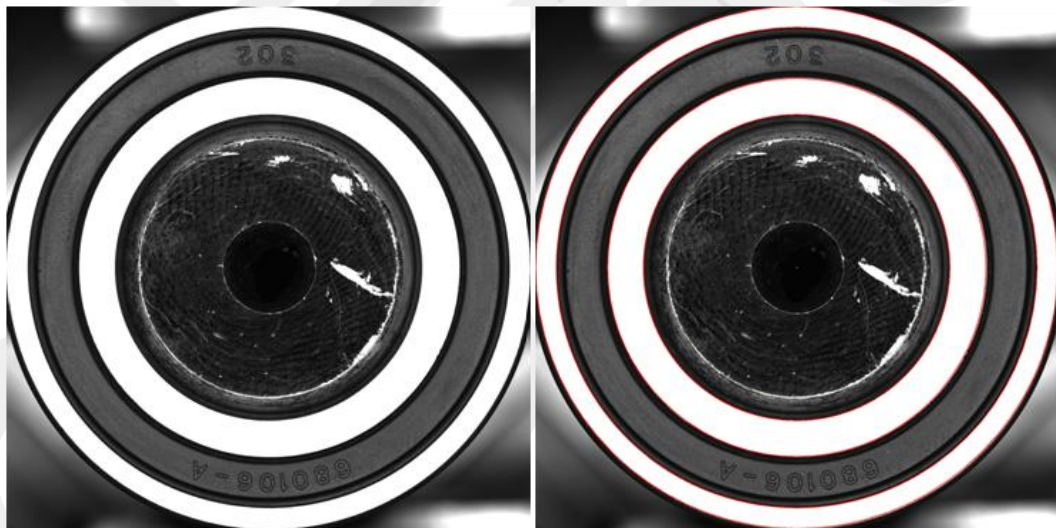
Figure 8: Crop and resize, (a) Original image. (b) Cropped image.

4.4. Hough Transform for Circle Detection

Similarly, assuming radius R is known, a circle in the x - y domain can be represented in the a - b domain as a point (a, b) :

$$\begin{cases} x = a + r\cos\theta \\ y = a + r\sin\theta \end{cases} \quad (1.2)$$

After detecting the edges in an image, for each point (pixel) at the edge, we draw a circle in the a - b domain. The point at which the highest number of intersections occurs is the center point [42 45]. By determining the center point, since the radius is already known, we can find the location of the circle in the image. If the radius is not known, then this process is repeated for each possible radius values that can be found in the image, see Figure 9.



(a) (b)
Figure 9: CHT result, (a) Cropped image, (b) CHT applied result image.

4.5. ROI Segmentation

Bearings vary widely according to their field of application and this leads to very complex surfaces being examined. Bearings can be designed with their own shape and special parameters. These parameters can be used to divide the fixing method on the bearing into different zones, see Figure 11 (a). A rubber seal is used on

the bearing being worked on and has an embossed marking on the rubber seal which includes the bearing type and seal's number, see Figure 10 (c).

Polar to Cartesian (P2C) conversion was used to convert the ring-shaped bearing image into a planar structure [42, 43]. R represents the outer radius of the outer ring, r the inner radius of the inner ring, W represents the length of the resulting planar structure, F represents the original image and D represents the targeted image, see Figure 10. The following equation is used for this translation:

$$\begin{cases} x = C_x + (r + R) * \cos(\theta) \\ y = C_y - (r + R) * \sin(\theta) \end{cases} \quad (1.3)$$

Where (C_x, C_y) is the center of bearing and (x, y) are the Cartesian coordinates corresponding to Polar coordinates (r, θ) .

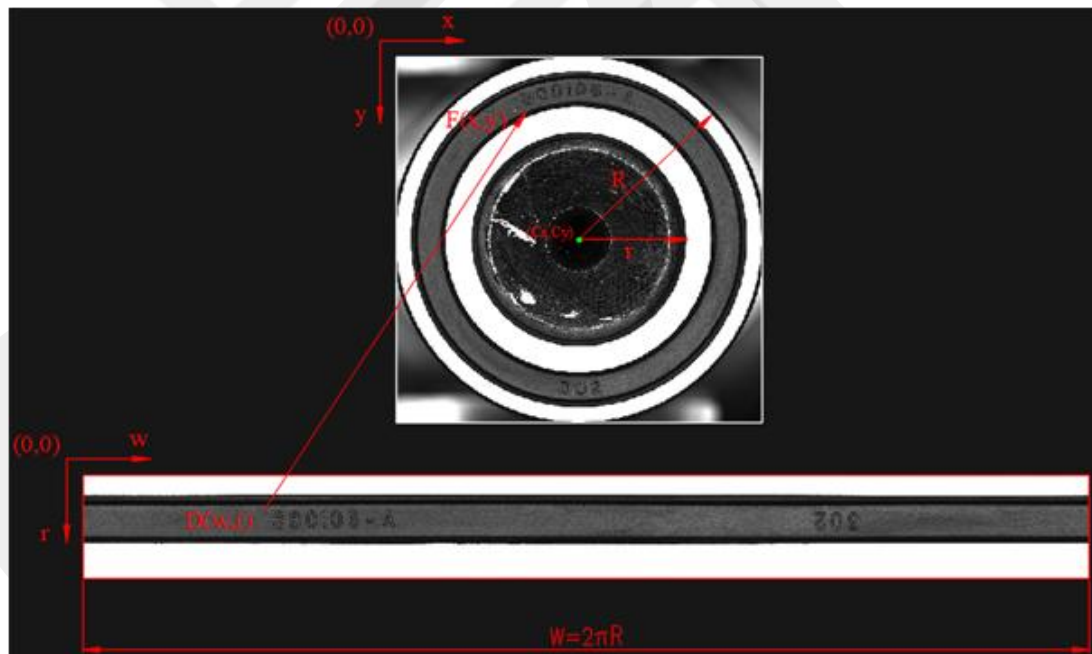


Figure 10: Polar to Cartesian conversion.

Detecting and distinguishing the bearing regions from each other enables us to work independently on each detected areas. This will make it possible to run defect detection operations on each region with different parameters. It will also be advantageous in facilitating the detection of specific defects and in increasing the accuracy of detection. The aim is to transfer the boundary coordinates to the

Cartesian coordinates so that the bearing's seal, inner ring and outer ring regions are completely separated from each other, see Figure 11.

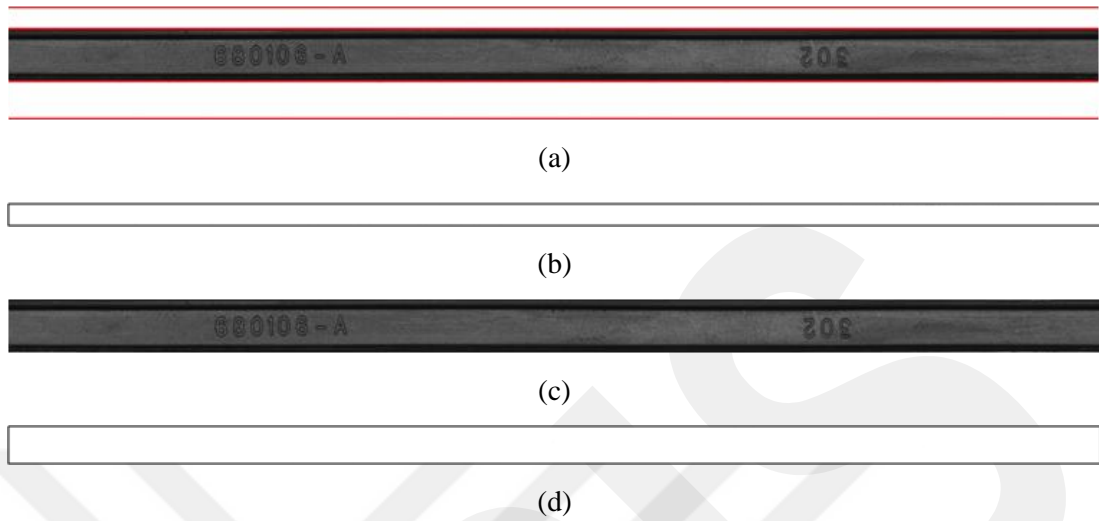


Figure 11: Image segmentation of bearings,(a) Segmentation results,(b) Outer ring, (c) Rubber Seal, (d) Inner ring.

4.6. Mean Value

Mean of an image is simply the arithmetic average of a 2D Vector [46]. In images, mean is the average intensity value of each pixel.

4.7. Standard Deviation

Standard deviation (STD) σ is defined as the square root of each pixels distance from the mean value [46]:

$$\sigma = \sqrt{\frac{\sum |x - \mu|^2}{N}} \quad (1.4)$$

Where x is the value of each pixel, μ is the mean and N is the number of pixels. Standard deviation gives a measure of how spread out/dispersed the values are from the mean.

4.8. Variance

Variance (σ^2) is closely related to standard deviation [46]. It is the average of the squared differences from the Mean. Variance is the square of standard deviation.

4.9. Skewness

Skewness is the degree of how differs the distribution is from the symmetrical [46]. Skewness is positive when the right side of the distribution plot is longer. In this state the mean and median are greater than the mode. Conversely, skewness is negative when the left side of the distribution plot is longer. In this state the mean and median are smaller than the mode. In the context of image processing, darker and glossier regions are more positively skewed than lighter and matter regions: this gives us a means to differentiate surfaces according to their skewness. The skewness of each pixel is the third standardized moment γ_1 :

$$\gamma_1 = E \left[\left(\frac{X - \mu}{\sigma} \right)^3 \right] = \frac{\mu_3}{\sigma^3} \quad (1.5)$$

Where μ is the mean, σ is the standard deviation, E is the expectation operator and μ_3 is the third central moment.

4.10. Kurtosis

Kurtosis gives us how much of the data is accumulated on the positive and negative extremes [46]. In other sense, it is related to the shape of the tails of the distribution. A high kurtosis (Leptokurtic) indicates that the data has heavy tails and a high amount of outliers. Conversely, a low kurtosis (Platykurtic) indicates all the values are accumulated in the center, it has a low amount of outliers. In another sense, kurtosis is a measure of difference the distribution is from the normal, with the Gaussian normal distribution having a kurtosis value of three. In the context of image processing, kurtosis is calculated from the histogram of the image and can be used for classification. The kurtosis of each pixel is the fourth standardized moment γ_2 :

$$Kurt[X] = E \left[\left(\frac{X - \mu}{\sigma} \right)^4 \right] = \frac{\mu_4}{\sigma^4} \quad (1.5)$$

Where μ is the mean, σ is the standard deviation, E is the expectation operator and μ_4 is the fourth central moment.

4.11. Median Filter

Median filter is also used for noise noise-reduction filtering [45]. In particular, it is widely used in reducing impact noise, known as “salt and pepper”. Each pixel value in the image is replaced by the median (middle value) of its neighbor pixel values. In order for the median filter to be applied, these pixels must first be determined and we provide this by creating a two-dimensional window in the x and y coordinates, also known as the kernel size. If the number of pixels entering the kernel is odd and multiples, the middle value is taken, but if there are even numbers and multiples, this time the average of the two remaining values is taken. Unlike the average filter, the median filter is protected in details while eliminating noise on the applied images. Thanks to this feature, it is used to filter out undesirable noise that may occur due to the fact that the bearing surface is not very homogeneous (multiple scratches on bearing surface approximately around) due to grinding process.

4.12. Gaussian Blur

Gaussian blur is a low pass filter used on digital images to reduce image noise and detail [45]. Visually, this creates a blur effect. In image processing it is primarily used to reduce noise, since most edge-detection algorithms are highly-sensitive to noise, the images are pre-processed with Gaussian blur. Mathematically, it is equivalent to convolving the image with a Gaussian function. Gaussian function defined in two dimensions is:

$$g(x, y) = \frac{1}{\sqrt{2\pi\sigma^2}} e^{-\left(\frac{x^2+y^2}{2\sigma^2}\right)} \quad (1.6)$$

Where (x, y) are the coordinates, the σ is the standard deviation.

4.13. Erosion and Dilation

Erosion and Dilation are the two operators used in mathematical morphology in which all other operators are derived from [47].

Erosion is used to “erode” the boundaries of shapes in binary or grayscale images. The visual effect is that the shapes become thinner and the holes inside become larger. The operation is similar to the Median filtering: each pixel value in the image is replaced by the minimum value of its neighbor pixels. An example application is separating intersecting/touching shapes from each other to use them. Also, subtracting the eroded image from the original one can be used as a edge detection method since the edges are eroded.

On the other hand, dilation can be seen as the opposite operator of erosion: each pixel value in the image is replaced by the maximum value of its neighbor pixels. The visual effect is that the shapes become larger and thicker while the holes inside get smaller.

The purpose of these morphological procedures in our study is to make visual defects more prominent and make them easy to detect. In addition, by means of these processes, it is to eliminate the characteristics of the surface in the structure which is not actually a visual defect.

4.14. Kullback-Leibler Distance

This method is inspired by our paper: “A. Mollaköy, E. Yengel and B. U. Töreyn, "Bearing fault detection method based on statistical analysis and KL distance," 2016 24th Signal Processing and Communication Application Conference (SIU), Zonguldak, 2016, pp. 1881-1884.”

In this study, histogram distribution plots were created over the image of the rubber seal region and Probability Density Function (PDF) [48] plots were calculated from these histogram data. Kullback-Leibler Distance (KLD) method [49, 50] was used to calculate logarithmic differences between the generated PDF graphics.

$$y = f(x|\mu, \sigma) = \frac{1}{\sigma\sqrt{2\pi}} e^{-\frac{(x-\mu)^2}{2\sigma^2}} \quad (1.7)$$

In the PDF formula, x represents the data set, μ is the average value corresponding to x , σ is the standard deviation corresponding to x . When calculating Gaussian's PDF graphs, mean value is accepted as zero ($\mu=0$) [48].

$$D_{KL}(P||Q) = \sum_i P(i) \ln \frac{P(i)}{Q(i)} \quad (1.8)$$

In the calculation of the KLD method used, $P(i)$ represents the instantaneous PDF value and $Q(i)$ represents the target PDF value.

4.15. Shifting Rolling Window

After all the methods have been applied on bearing images divided into ROI regions and converted to Cartesian coordinates, they have been made ready for defect inspection. In case of visual defects on images prepared for defect inspection in binary format, it is aimed to display the related defects as black and the remaining surface as white. After making sure that this is achieved on images in binary format, the sliding window method is proposed for defect detection.

In this technique, first of all, a two-dimensional filtering window known as the kernel is created in order to perform defect scanning of the images. It is suggested that all of the filtering variables within this window should be one. Because the working principle of the proposed method; the new value is calculated by multiplying each variable in the binary format that corresponds to the window with one, and these new values are added. The next step is to divide the calculated

values by kernel size and multiply the resulting value by 100. This will give us a percentage. When it comes to defect detection, the result is equal to the kernel size if all the values in the window are equal. This means that the resulting result is 100%, i.e. there is no visual defect on the surface position at which the window momentarily coincides. In the other scenario, values are zero in the region with visual defect. When the two-dimensional sliding window comes to these regions, the total decrease will be experienced as a result of the operations performed. The decrease in the total value will also decrease the percentage value. Any decrease in the percentage indicates that the region has a visual defect [51].

According to the experience obtained from real-time tests, a threshold value specific to different visual defects was determined. If the calculated instantaneous value falls below this determined threshold value, it means that the examined bearing is a visually defective bearing. In addition, the most important of the awareness acquired is related to the window size. The smaller the sliding window size is selected, the more inversely it increases the sensitivity of the proposed method. As a result, different window sizes and threshold values were independently determined for each type of defect to improve the accuracy of the defect detection.

CHAPTER 5

EXPERIMENTAL RESULTS

5.1. Adaptive Thresholding

Both the factory environment and the lighting systems used may be subject to varying lighting conditions. As a result, problems may arise during the operations necessary for the positional fixation of the bearing on the image. In order to take action against this scenario, the variable light environment is created in a controlled manner and the bearing images are captured, see Figure 12. In order to develop software that can adapt to this scenario, the relationship between light intensity and threshold value has been examined, see Figure 13. The main purpose of determining threshold values suitable for variable light conditions is to ensure that the pre-processing of bearing images (separation from background, Hough Transform etc.) is smooth and work correctly in all conditions.

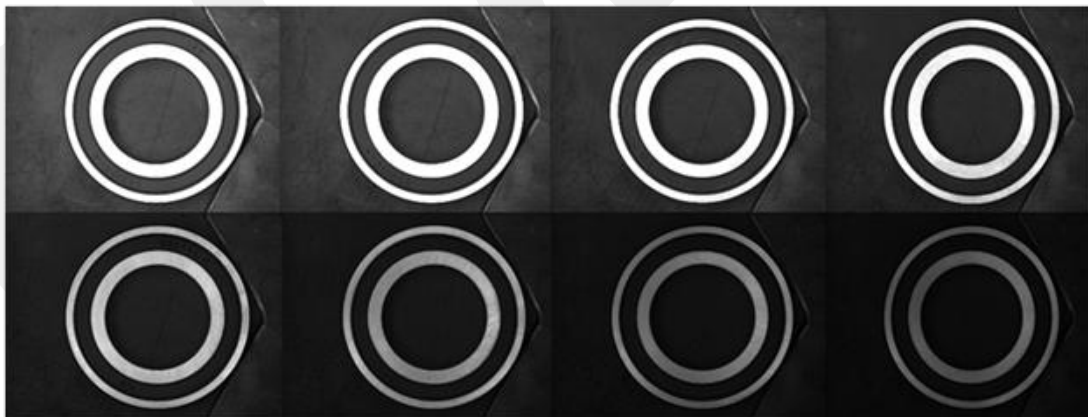


Figure 12: Examples of bearings illuminated with varying light intensities.

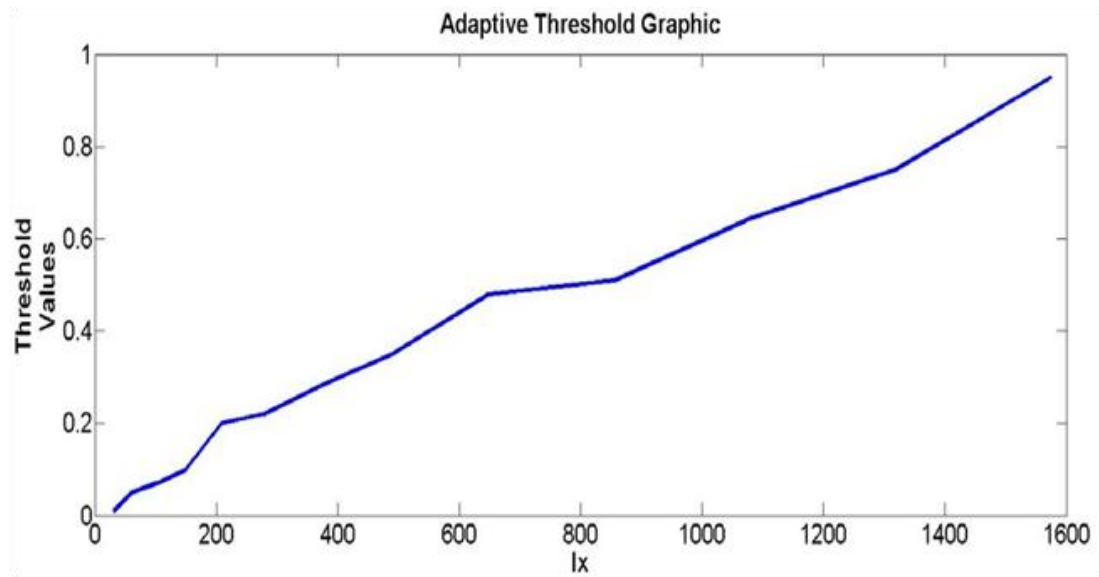


Figure 13: Relationship between Light Intensity (lux) – Threshold value

By locating the bearing images to be examined on the image, the bearing is distinguished from the background so that only the region (bearing) to be examined remains in the image. The cutting of the image of the bearing distinguished from the background intact and the resizing of the cropped part is arranged taking into account the depth of field.

As a result, with this experimental study, a system design that can adapt to variable light conditions will be made. However, the VisiBear system, designed as a result of the experience gained, is designed to minimize the occurrence of variable light conditions. Thus, the adaptive threshold value is no longer needed.

5.2. Mean, STD, Skewness, Kurtosis and Variance

Missing rubber seal and reversely assembled rubber seal defects are formed in the seal region as ROI. Since these defects are very obvious types of visual defects, they can be provided with basic mathematical operations to be detected, see Table 3.

Table 3: Mathematical results of the defect types of seal.

12V-625mA/1575lx					
6806 TypeBearing	STD	Mean	Skewness	Kurtosis	Variance
Properly assembled	4.4049	69.8685	-0.2046	2.1383	20.0630
Reversely assembled	6.1968	71.5107	-0.3078	2.6913	38.6988
Missing rubber seal	16.7616	111.4279	0.9921	3.8626	284.2180

As can be seen from the results given in Table 3, bearing with the missing rubber seal can be easily separated from all methods. The property variance value is the most ideal defect separation method when compared with the other results. On the other hand, it is not possible to make a healthy defect determination for bearing with reversely assembled.

5.3. KLD Results

In the next step, average histogram distributions were obtained by using 10 images from each bearing group. The zero-mean PDF graphs were extracted from these mean histogram values and the probability values on the mean PDF graph were used as target probability values. The probability values of the images belonging to each of the bearing groups (defect-free, reversely assembled rubber seal, missing rubber seal) were calculated. The difference between the calculated target probability values and instant PDF values (Kullback-Leibler Distance) values were found. If the calculated KLD value of each new sample is close to the target probability value, it is provided that the bearing examined belongs to that group.

Reversely assembled rubber seal defect type can be determined precisely and especially in order to support defect detection with variance value, the method mentioned in section 4.13 has been applied. The result of the method is shown in Figure 14.

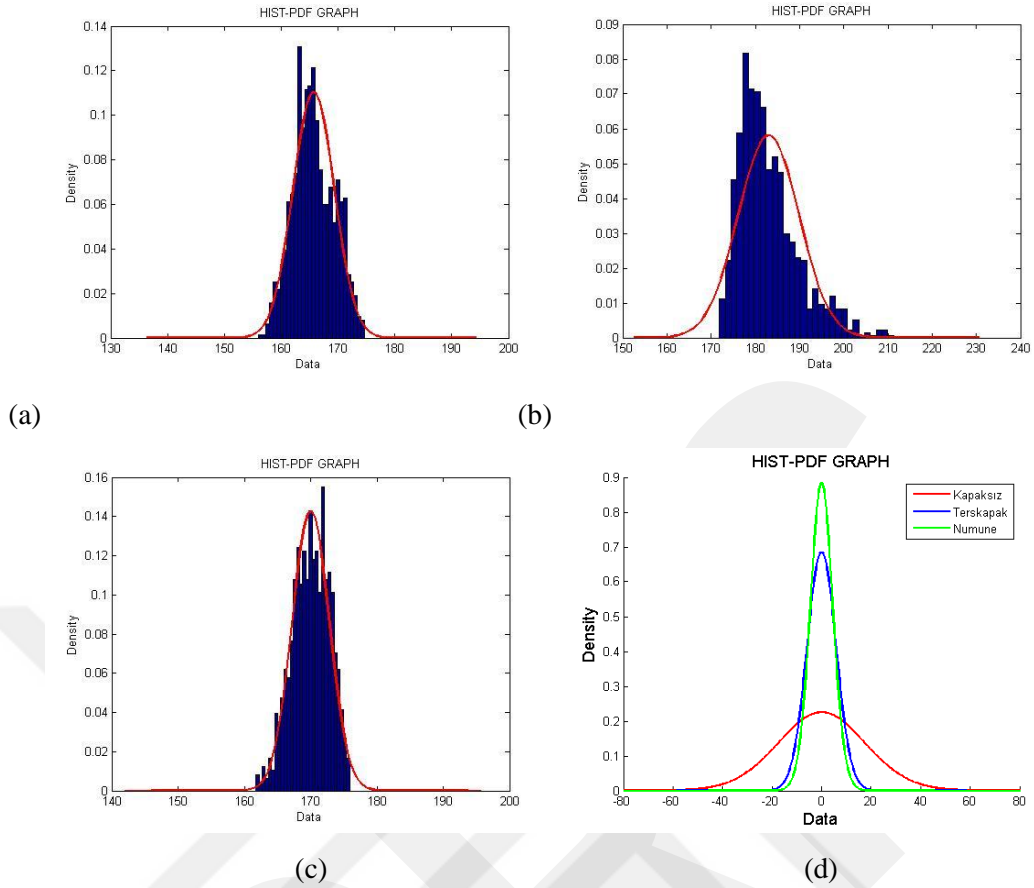


Figure 14: KLD results,(a) Histogram-PDF graph of reversely assembled seal, (b) Histogram-PDF graph of missing rubber seal, (c) Histogram-PDF graph of properly assembled rubber seal, (d) Normal PDF graphics of these bearing samples.

5.4. Power Graphs Results

A faster detection method has been studied to support the proposed method. Power graphs are calculated for visual defect scenarios where the bearing seal is not mounted (missing rubber seal) or the seal is mounted reversely [52]. When these defect types and the properly assembled bearing were evaluated together, all visual details were found in the middle part of the seal's region. Therefore, a single line was taken to correspond to the middle part of the gray scale seal images with scale values of 0-255 (8 bits). This created a new vector of $1 \times W = 2\pi R$ (W = width of bearing on Cartesian coordinates). The graph containing the pixel values of this vector is shown in Figure 15(a) as "raw data. A 1×2 high-pass filter was applied to highlight the details on the image (sudden pixel value changes), see Figure 15(b). The absolute value was taken to filter the negative values that occurred after filtration, see Figure 15(c). All these operations are visualized from using the reversely assembled seal

bearing data, because the reverse seal's surface is completely homogeneous. Figure 15(c) shows that the maximum peak remains at the four bands after all operations. All of these methods have been applied to the mentioned these defect types. Finally, the standard deviation value was calculated from the vector data whose absolute value was taken and a threshold value was found by taking four times the calculated value. When the threshold value is applied, it is observed that the data of the reversely assembled seal is reduced to zero band, peaks are occurs at the parts corresponding to the balls from the missing rubber seal's data and in the relief embossed marks of the properly assembled. The comparative power graphs of these data are shown in Figure 15(d), and this power graph provides a defect classification between missing rubber seal and reversely assembled defect types [52].

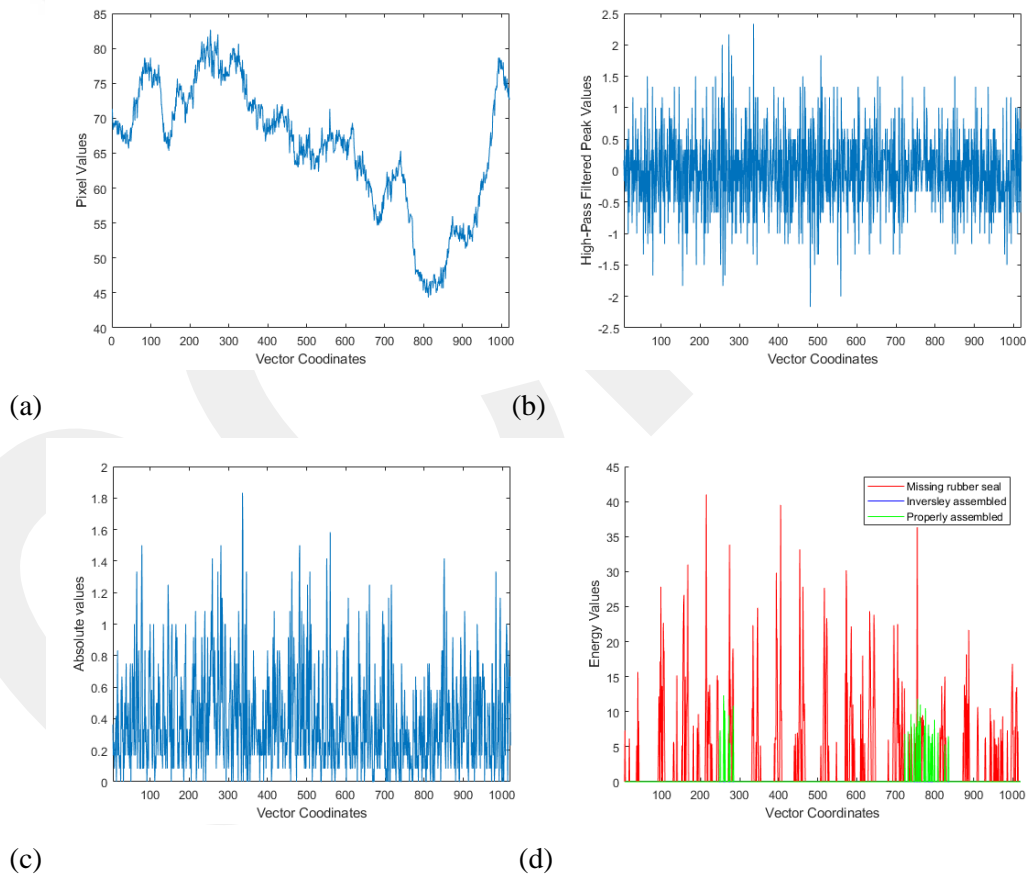


Figure 15: Power graph's results,(a) Raw data, (b) High-Pass filtered data, (c) Absolute values from High-Pass filtered data, (d) Comparative data with threshold value applied.

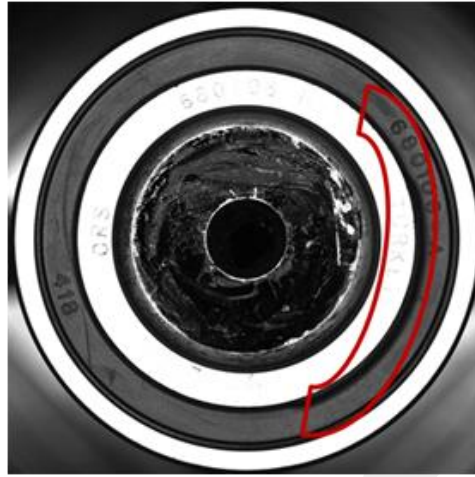
5.5. Sliding Rolling Window Results

Once the reversely assembled and missing rubber seal defects have been successfully detected, other defects that may occur on the bearing seal areas can be detected. In order for other visual defects to be detected correctly, the seal's binary image must be constructed in such a way that only the defect remains.

5.5.1. Rubber Seal's Defects

5.5.1.1. Overlap on Rubber Seals

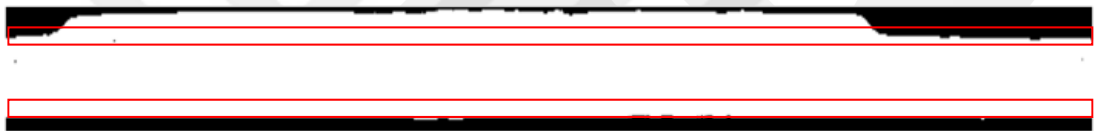
The first type of defect is the type of visual defect that occurs when the lips of the lids do not fit into the inner ring seal groove and curl outward, see Figure 16 (a). The seal image, converted to Cartesian coordinates and divided into ROI regions, is converted to binary format by thresholding. For the detection of these defects, firstly the parts of the lid lips on the lid which are at the inner ring and outer ring boundaries are determined as ROI for defect inspection, see Figure 16.



(a)



(b)



(c)



(d)



(e)

Figure 16: Overlap defect detection, (a) Bearing sample with Overlap defect, (b) Cartesian coordinates, (c) ROI of defect inspection, (c) Inner rubber seal's lip, (d) Outer rubber seal's lip.

When the window created in the sliding rolling window method coincides with the black regions (visually defective) that occur in Figure 16 (d), the percentage value will decrease and thus the defect is determined.

5.5.1.2. Deformation on Rubber Seals

The second type of defect is that the seal can be deformed due to the application of high force by the press machine during seals assembly. This deformation can cover the entire surface or can only be localized, see Figure 17 (a). The seal image, converted to Cartesian coordinates and divided into ROI regions, is converted to binary format by thresholding. These defects usually occur in the central region of the seal. The middle region for this determination is taken as ROI, see Figure 17 (c).

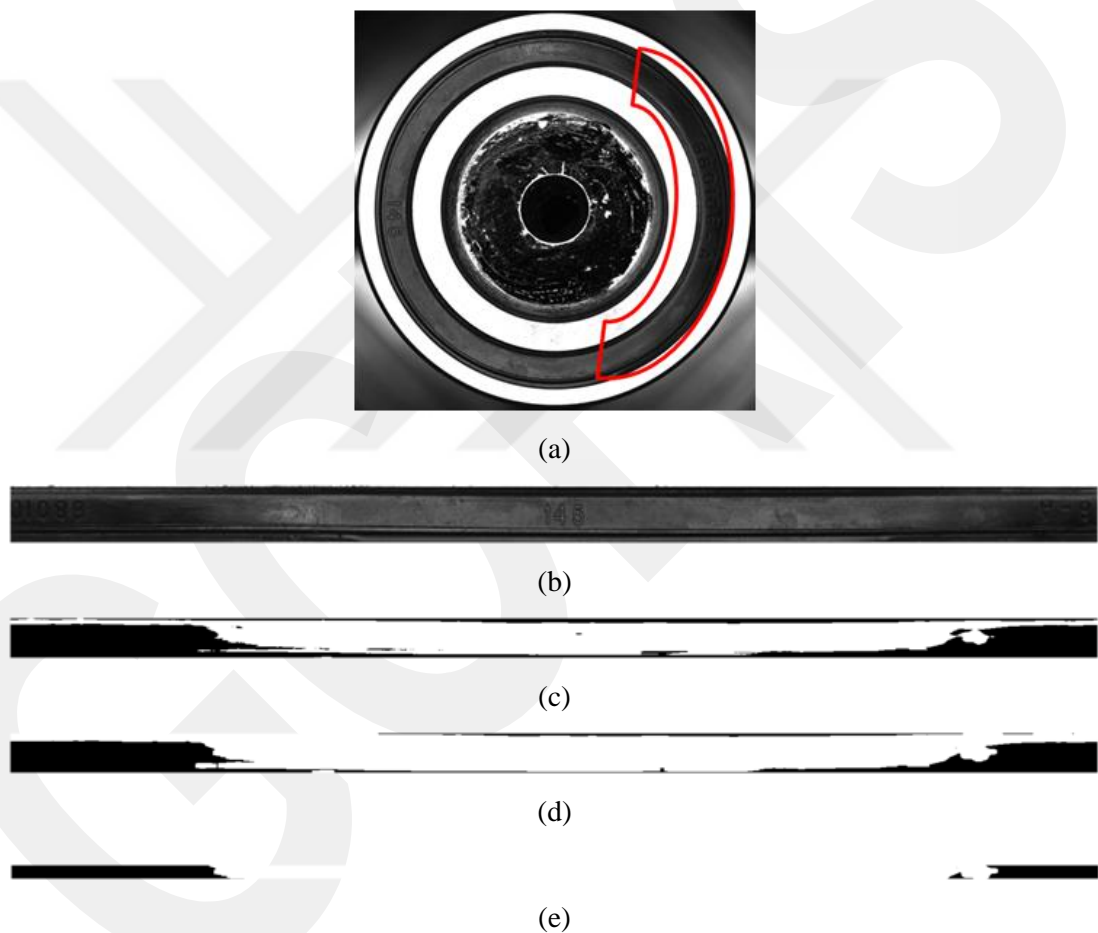


Figure 17: Deformation defect detection, (a) Bearing sample with deformation defect, (b) Cartesian coordinates, (c) Binary transformation image, (d) Erosion/dilation applied image, (e) ROI of defect inspection.

The ROI here is critical because it corresponds to the part with the embossing marks on the seal. It is very important that embossed marks are not detected as defects. Therefore, erosion / dilation processes have destroyed these marks, see

Figure 17 (d). When the window created in the Sliding rolling window method coincides with the black regions (visually defective) formed in Figure 17 (e), the percentage value will decrease and thus defect detection will be provided.

5.5.1.3. Scratch on Rubber Seals

The last of these types of defects can cause scratches on the surface during the installation of the press machine rubber seal, see Figure 18 (a). All operations described in Section 5.5.1.2 apply to this type of defect. These defects generally occur in the central regions of the closure and the central region for this inspection is taken as ROI, see Figure 18 (c).

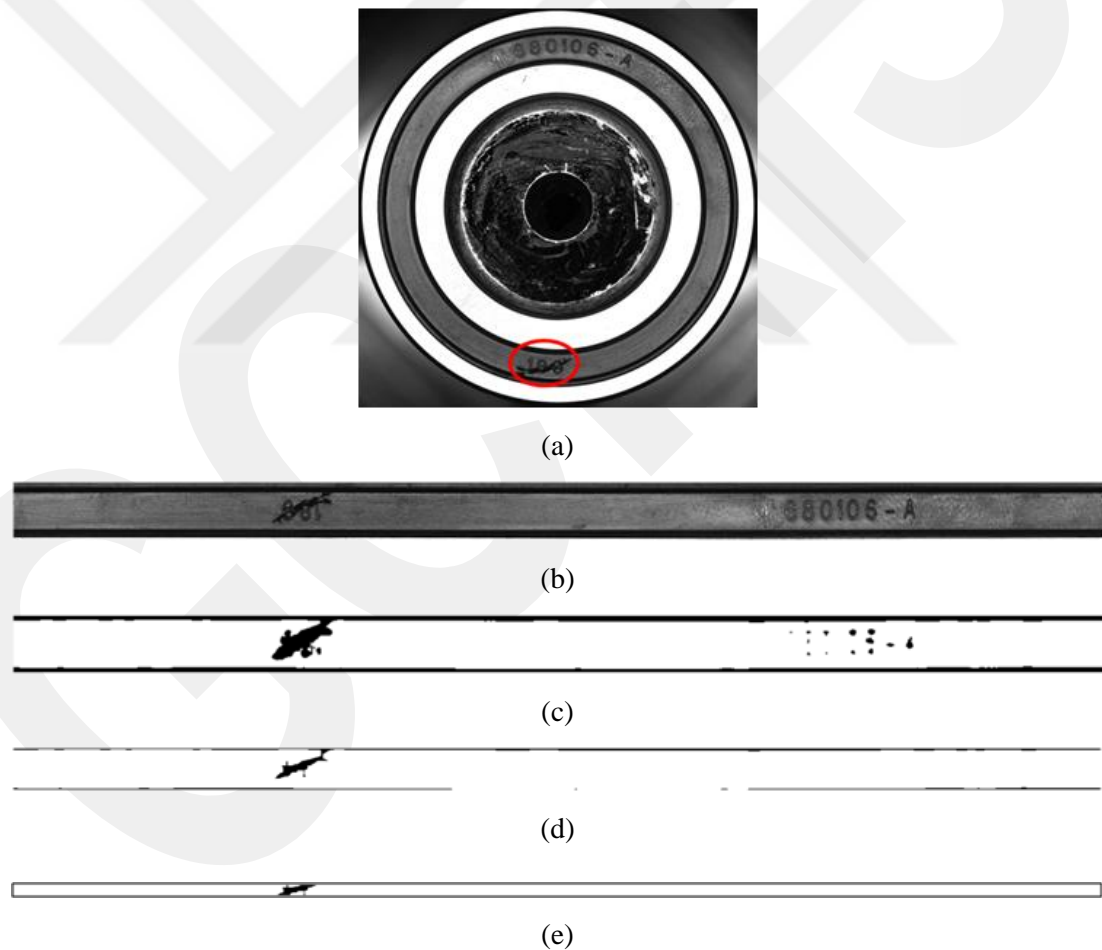


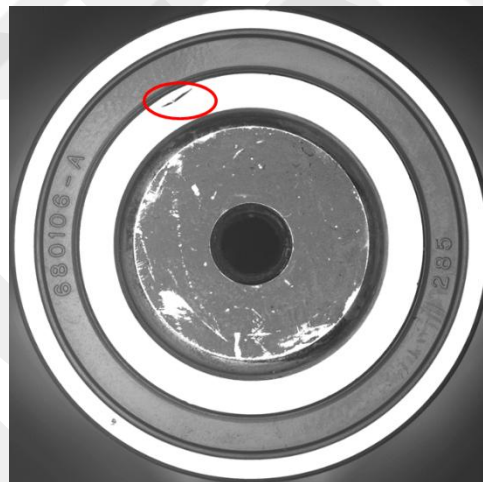
Figure 18: Scratch defect detection, (a) Bearing sample with scratch defect, (b) Cartesian coordinates, (c) Binary transformation image, (d) Erosion/dilation applied image, (e) ROI of defect inspection.

It is very important that the embossed brands on the seal are not detected as defects. Therefore, erosion / dilation processes have destroyed these marks, see Figure 18 (d). When the window created in the sliding rolling window method coincides with the black regions (visually defective) that occur in Figure 18 (e), the percentage value will decrease and thus the defect is determined.

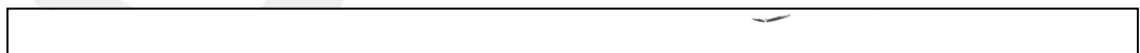
5.5.2. Face Defects

5.5.2.1. Scratch on Face

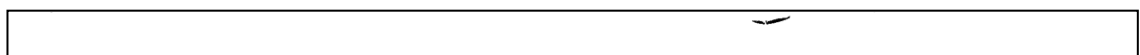
These are the visual defects that occur in the metal regions of the bearing called the surface. The first defects types are scratch on the metal face, see FIG. Figure 19 (a). All operations described in Section 5.5.1.2 apply to this type of defect. These defects usually occur in the face regions of the inner / outer ring and the rings are taken as ROI for this examination, see FIG. Figure 19 (c).



(a)



(b)



(c)

Figure 19: Scratch defect detection on face,(a)Bearing sample with scratch defect on inner face, (b)Cartesian coordinates on grayscale, (c)Binary transformation image and also ROI of defect inspection.

When the window created in the sliding rolling window method coincides with the black regions (visually defective) that occur in Figure 19 (c), the percentage value will decrease and thus the defect is determined.

5.5.2.2. Impact on Face

These are the visual defects that occur in the metal regions of the bearing called the surface. The second defects types are impact on the metal face, Figure 20(a). All operations described in Section 5.5.1.2 apply to this type of defect. These defects usually occur in the face regions of the inner / outer ring and the rings are taken as ROI for this examination, see Figure 20 (c).

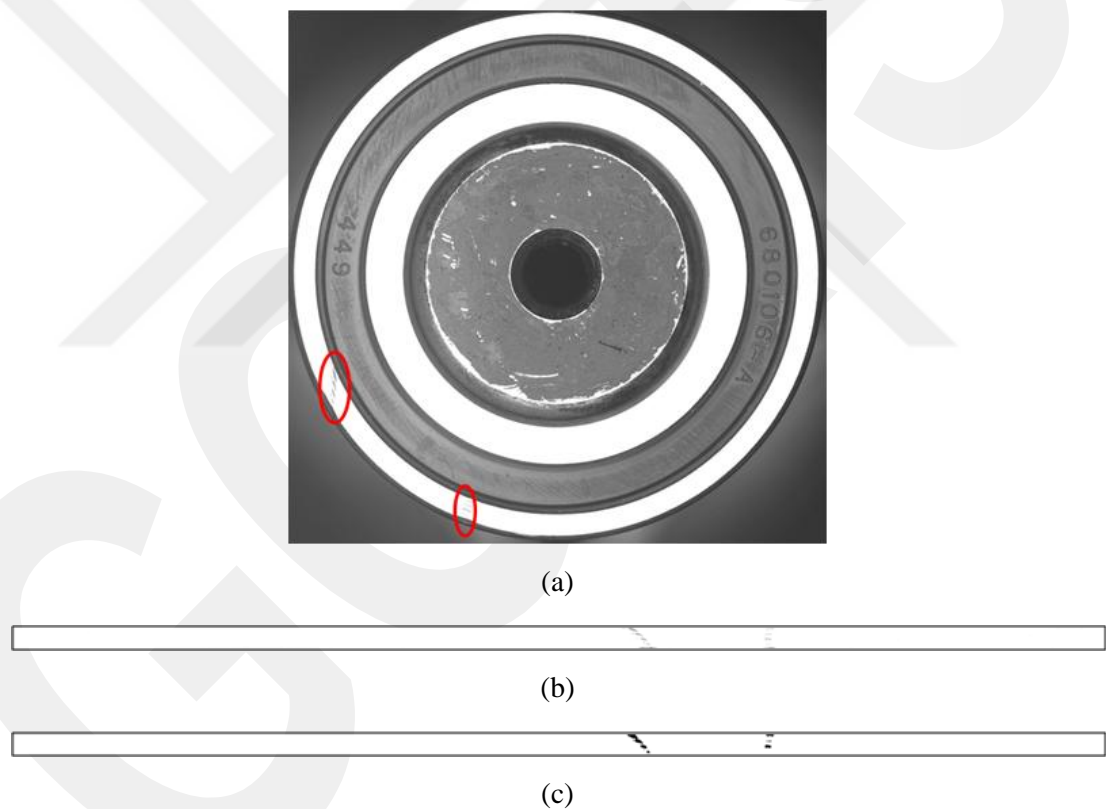
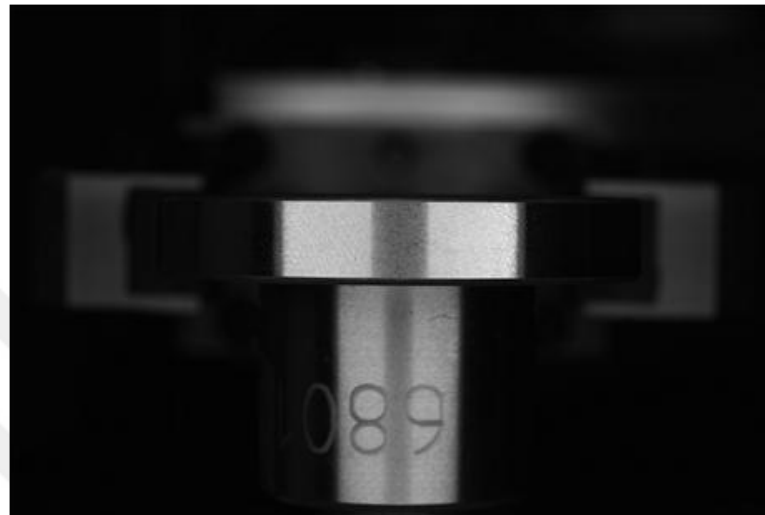


Figure 20: Scratch defect detection on face, (a) Bearing sample with impact defect on inner face, (b) Cartesian coordinates on grayscale, (c) Binary transformation image and also ROI of defect inspection.

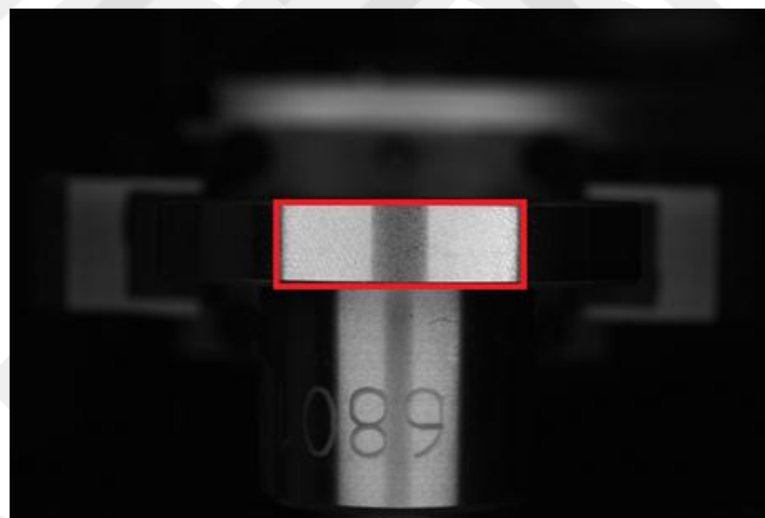
When the window created in the sliding rolling window method coincides with the black regions (visually defective) that occur in Figure 20 (c), the percentage value will decrease and thus the defect is determined.

5.5.3. Outer Diameter Defects

Contrary to all the studies performed, the acquisition operations described at the 4th station turn the bearing and capture multiple images to capture the whole environment, see Figure 21.



(a)



(b)

Figure 21: Scratch defect detection on face,(a) An exemplary outer diameter bearing image.

(b) The brightest parts of the image in question are determined by Otsu thresholding, subjected to expansion morphological processing and marked with the method of connected components to obtain the smallest spanning box.

5.5.3.1 Rust Defects on Outer Diameter

The specific type of error is presented in Figure 22. In order to detect such defects, Gaus filtering was applied to the image, which is a kind of low pass filtering. Thus, small / short traces that are structurally found on the outer diameter and which can be mixed with rust zones under existing lighting are eliminated. The process is shown in Figure 23. Thus, Gaus Adaptive Filter (GAF) is performed on the hazy image and the rusty regions can be detected as shown in Figure 24. Sliding operations are performed on the detected image, resulting in image defects resulting from the inclination of the outer diameter, see Figure 25. As a result, only the areas with rust defects are obtained. Finally, by defining a 32x32 frame, this frame is shifted over the image and the percentage of black pixels remaining within the frame is calculated. As seen in Figure 26, the frames found to be more than one hundred are recorded and rusty regions are detected.



Figure 22: ROI with rust defect on the outside diameter.

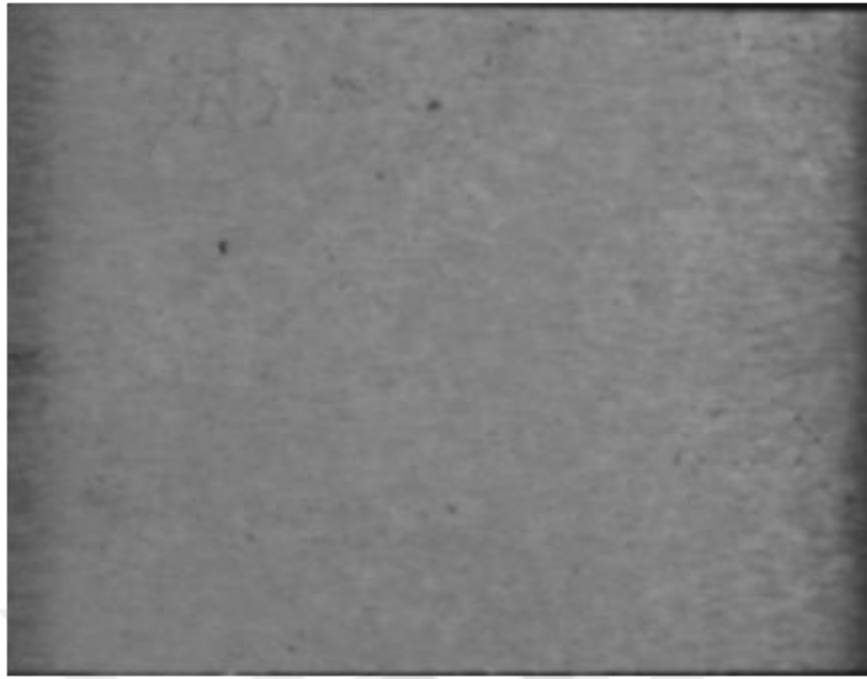


Figure 23: Gaussian Blur image and median filter are applied on rust ROI.

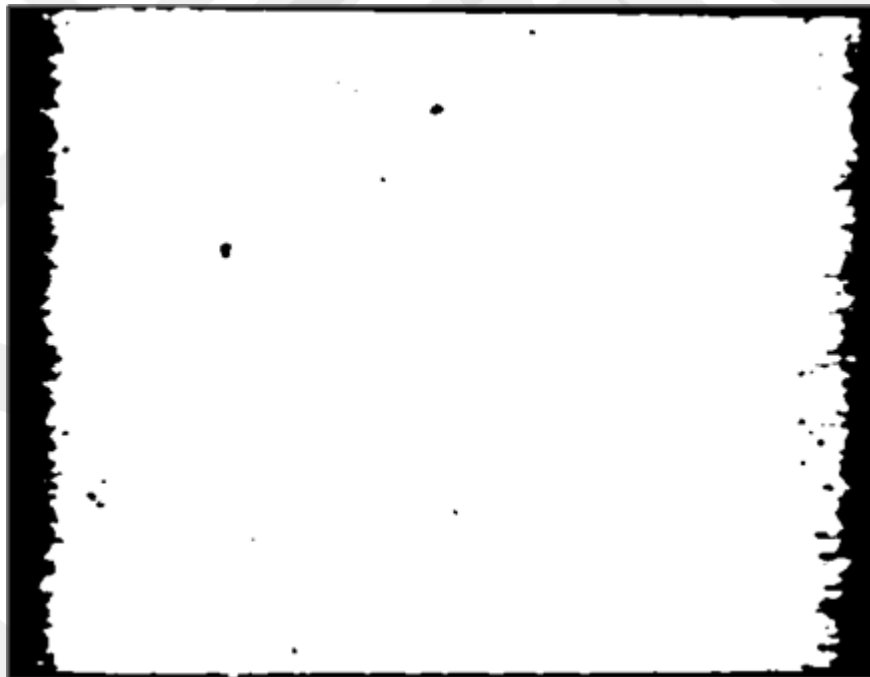


Figure 24: Binary transformed image on rust ROI.

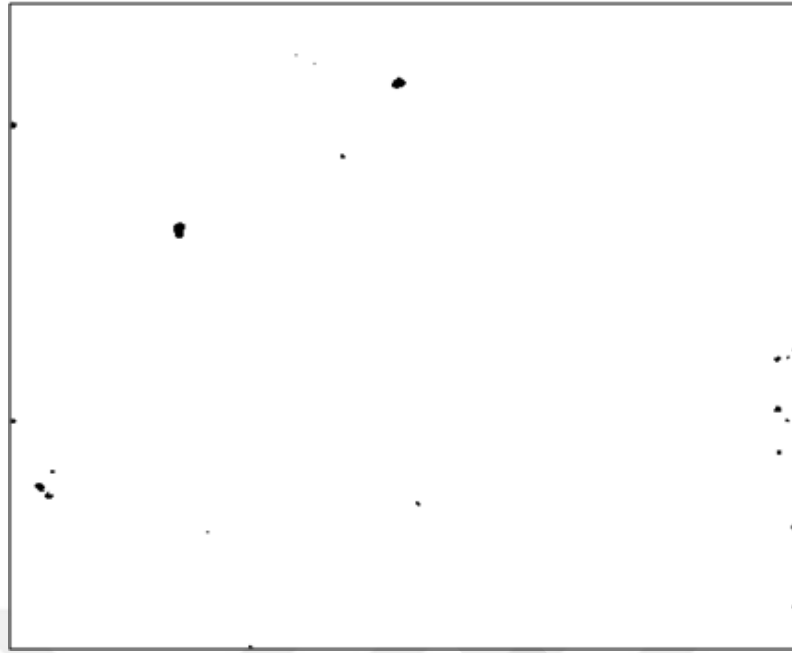


Figure 25: Cropped and resized image on rust ROI for defect detection.



Figure 26: 32x32 frame results in a bearing with rust defects on outer diameter.

5.5.3.2. Shoe Trail Defects on Outer Diameter

Another type of visual defect seen on the outer diameter is the shoe trail defect. This defect type appears as horizontal tracks on the outer diameter. The smooth outer surface of the outer diameter surface, the same amount of illumination under the brightness of the surface according to the slope of the region creates a change, see Figure 27 and 28. Similar to the rust defect, the image is softened by Gaussian filtering and is shown in Figure 29. Then, as shown in Figure 30, Otsu Thresholding method is applied and shoe trail defects are made clear. As shown in Figure 31, similar to the removal of the first external diameter defect after the Crop/Resize operation, it is determined based on the average and standard deviation brightness values of the smooth bearings. For this purpose, the average brightness values are calculated over 32x32 regions on the region of interest. If these values are different from the mean brightness value obtained from the problem-free regions by the two standard deviations, these regions are determined after the morphological processes and the associated component analysis steps. As a result, the defects detected by the 32x32 frame are shown in Figure 32.

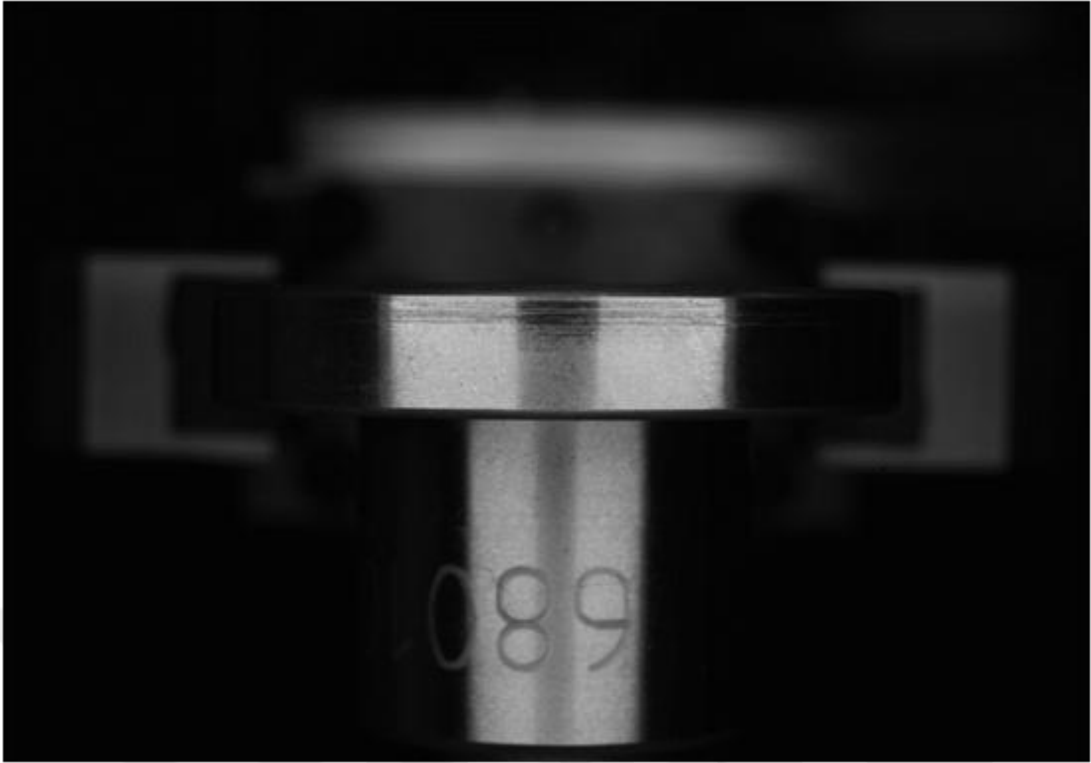


Figure 27: Example of a bearing with shoe trail defect on the outside diameter.

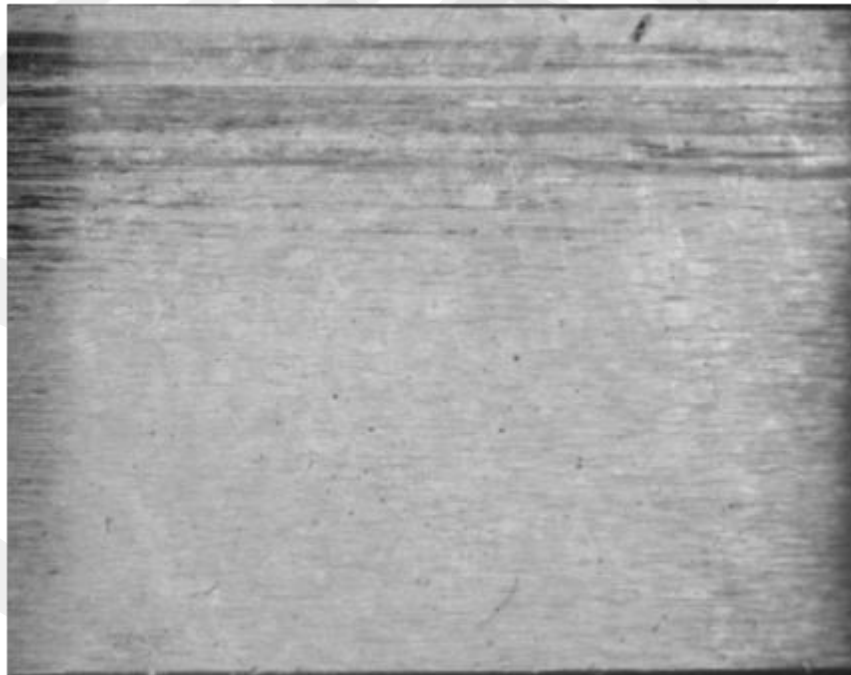


Figure 28: ROI with shoe trail defect on the outside diameter.

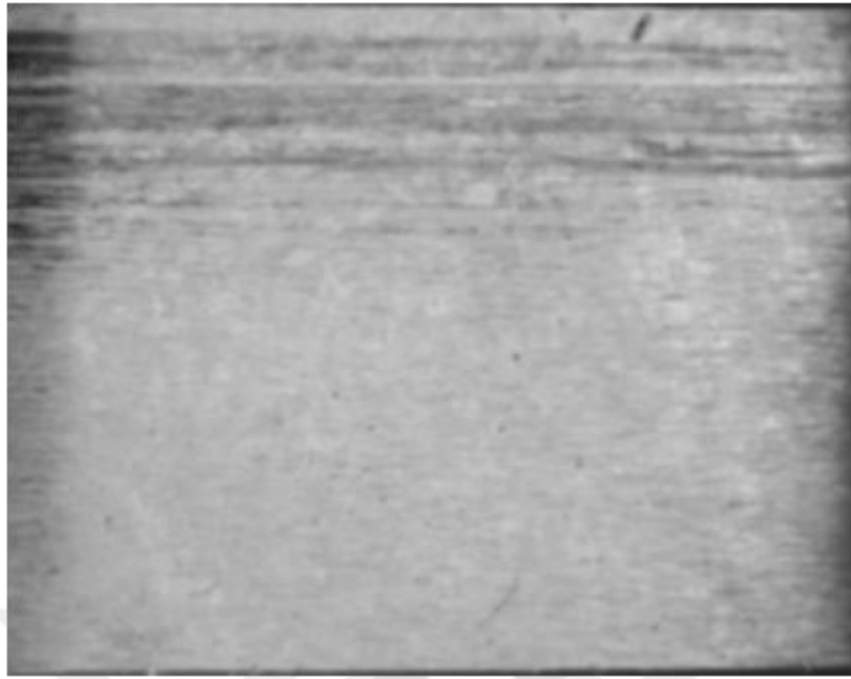


Figure 29: Gaussian Blur image and median filter are applied on shoe trail ROI.

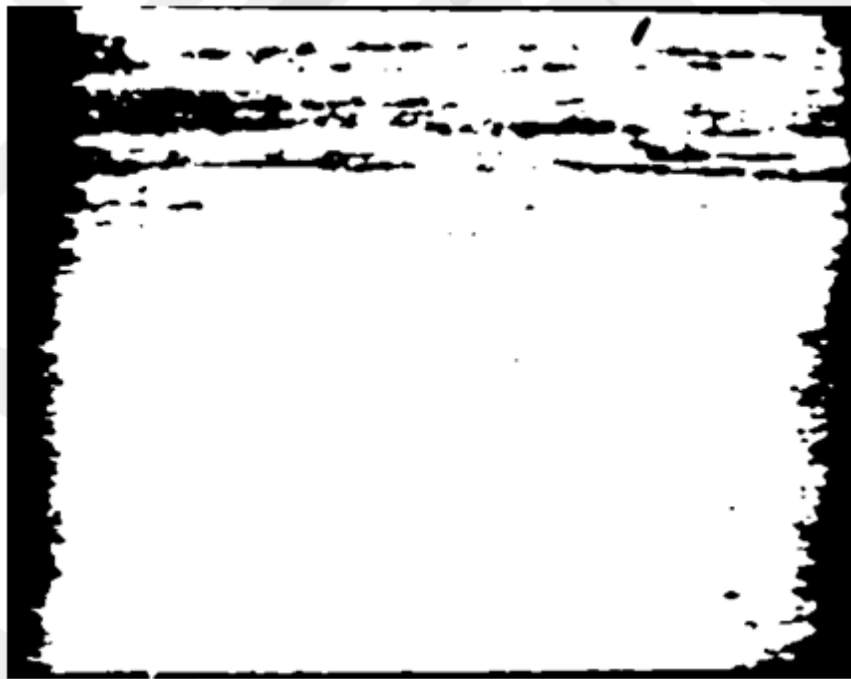


Figure 30: Binary transformed image on shoe trail ROI.



Figure 31: Cropped and resized image on shoe trail ROI for defect detection.



Figure 32: 32x32 frame results in a bearing with shoe trail defects on outer diameter.

5.5.3.3. Impact Defects on Outer Diameter

For this defect, examples are shown in Figure 33 and 34. For the purpose of identifying these defects, first of all, the brightest regions containing the reflection of the light source in the pictures taken for the outer diameter are determined and marked by thresholding and connected component analysis. Then, the erosion/dilation method is used in both the detection of rubber surface defects and the detection of metal surface defects in these regions. Thus, it has become possible to detect rust and impact / scratch / scratch defects at different scales and sizes.

Another approach developed in this period for finding rust regions is based on median filters, see. According to this approach, the region of interest is passed through a 5x5 median screen, see Figure 35. If there is no rust in the ROI, the difference between the original image and the filtered image is negligible. Then, as shown in Figure 36, Otsu Thresholding method is applied and impact defects are made clear. As a result, the defects detected by the frame are shown in Figure 38.

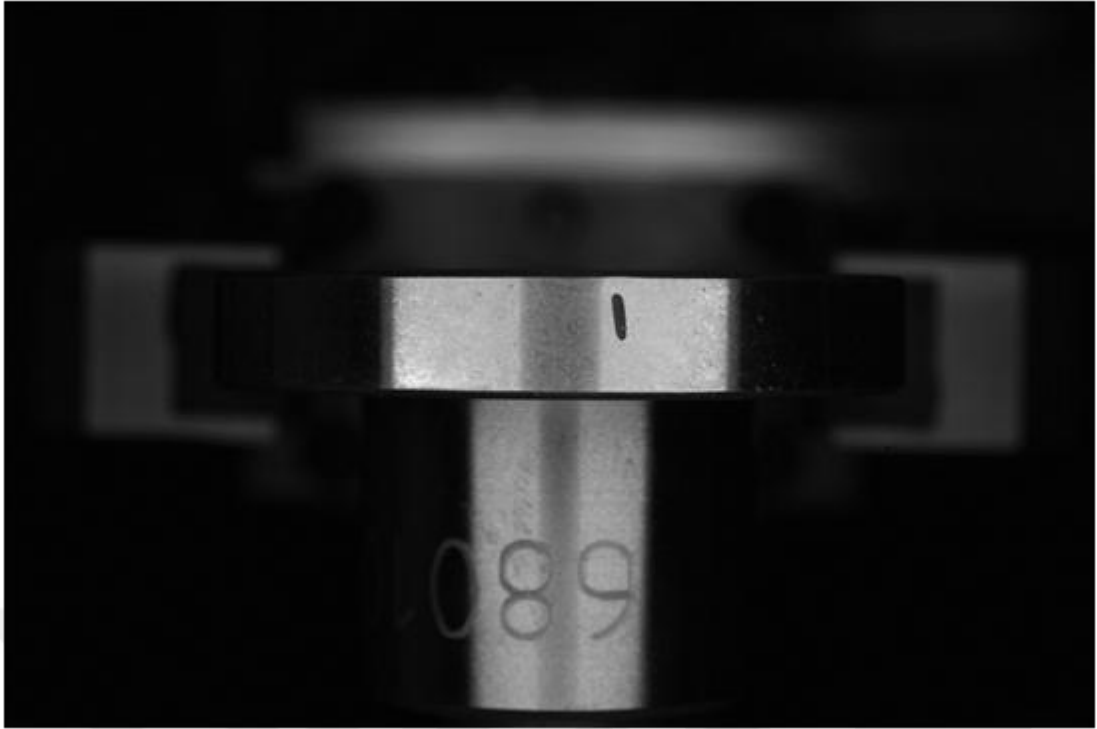


Figure 33: Cropped and resized image on impact ROI for defect detection.

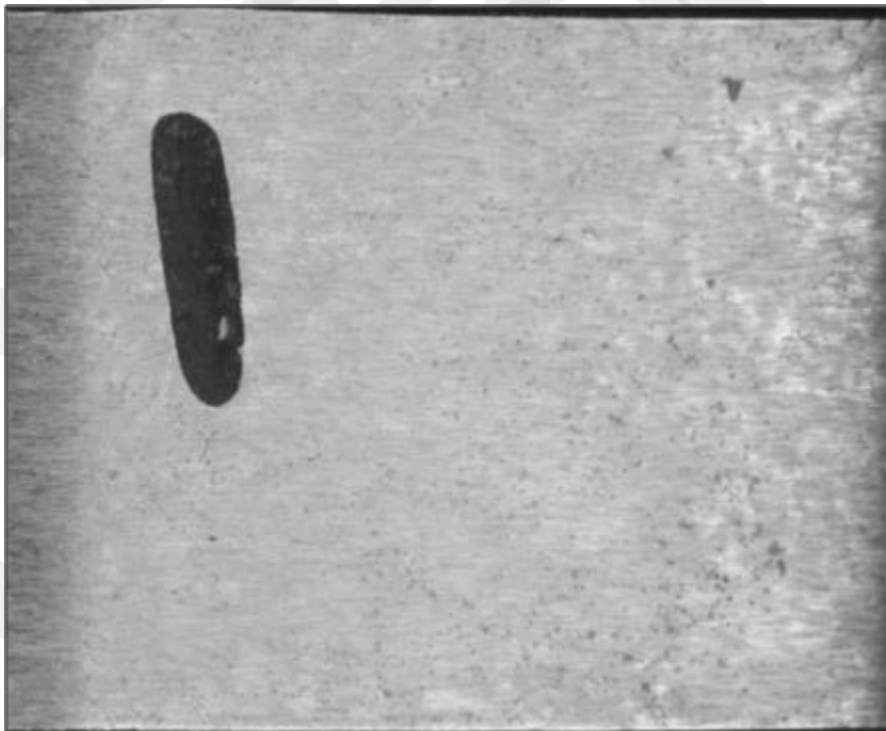


Figure 34: ROI with impact defect on the outside diameter.

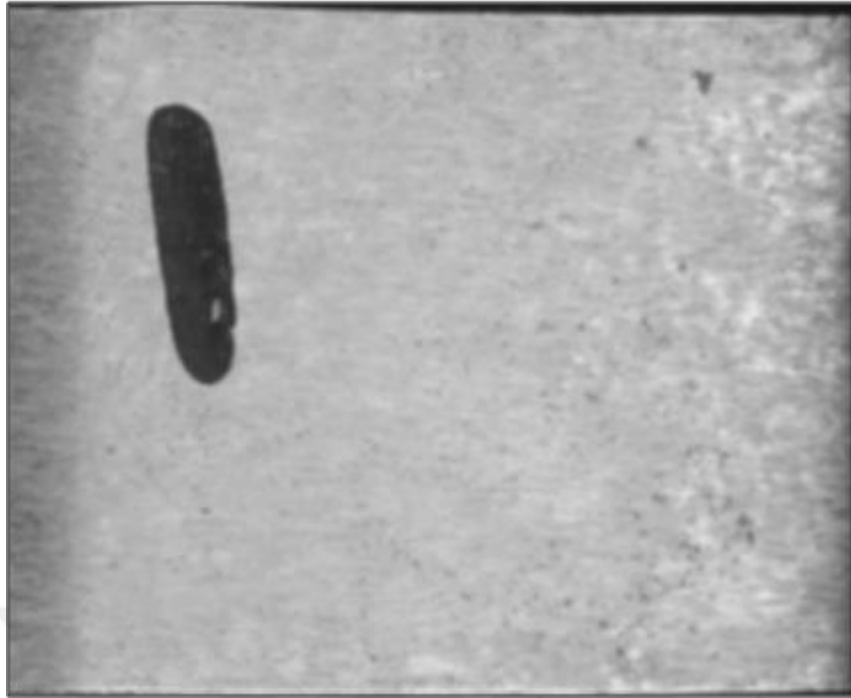


Figure 35: Gaussian Blur image and median filter are applied on impact ROI.

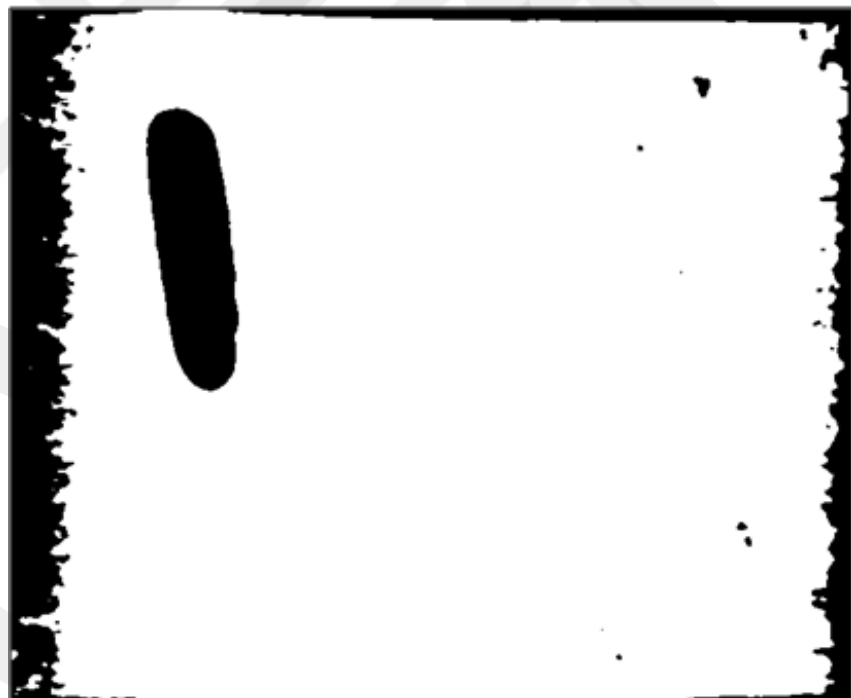


Figure 36: Binary transformed image on impact ROI.

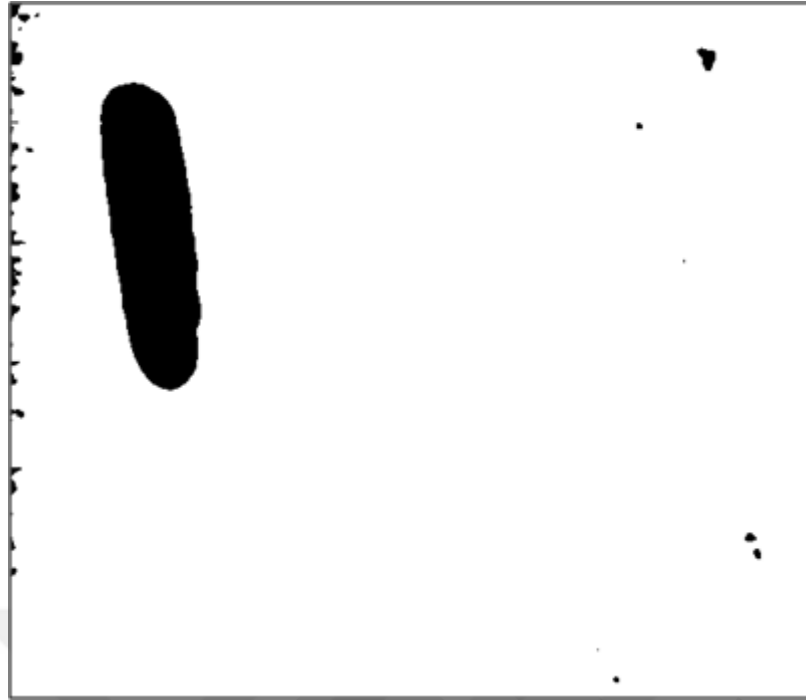


Figure 37: Cropped and resized image on impact ROI for defect detection.



Figure 38: 32x32 frame results in a bearing with impact defects on outer diameter.

5.6. Confusion Matrices

The applicability of the proposed methodology on the VisiBear system must be measurable. When all defect control stations were evaluated together, a total of 1172 samples were examined. These include 262 defect-free, 100 reversely assembled rubber seals, 200 missing rubber seals, 65 deformations, 36 overlap, 221 scratches (both on rubber seal and metal surface), 158 impacts, 106 rusts and 24 shoe trails. The performance measurability of the designed system was achieved by calculating the accuracy rates. [Accuracy]. The formulation of accuracy is;

$$A_{cc} = \frac{TP + TN}{P + N} * 100\% \quad (1.9)$$

Where TP is the number of defect-free samples that are correctly recognized, TN is the number of defective samples that are correctly rejected, P is the total number of defect-free samples, N is the total number of defective samples.

The results on RSIS are shown in Table 4. A total of 690 samples were inspected at this station, of which 490 were rejected from production by VisiBear. Among the 490 bearing examples that were rejected, there were 488 actual bearing defects. In other words, the samples rejected at the first station include 2 defect-free bearings. Specifically, 2 defect-free samples were rejected from the mass production as classified as overlap defect by the system. In addition, 2 pieces of bearing samples with overlap defects could not be detected by the system and were not removed from production. Accordingly, the accuracy of the RSIS is 96.9%.

Table 4: Confusion matrix of the inspection results of the first inspection station.

Actual class	Predicted class							Number of samples
	Defect free	Reversely Assembled	Missing RS	Deformation	Overlap	Scratch		
Defect free	198	0	0	2	0	0	200	
Reversely Assembled	0	100	0	0	0	0	100	
Missing Rubber Seal	0	0	200	0	0	0	200	
Deformation	0	0	0	62	3	0	65	
Overlap	2	0	0	0	30	4	36	
Scratch	0	0	0	0	10	79	89	
Total	200	100	200	64	43	83	690	
Accuracy	$(198+100+200+62+30+79)/690 = 96.9\%$							

The results on FIS are shown in Table 5. A total of 405 samples were examined at this station, 216 of which were rejected from production by VisiBear. Among the 216 bearing examples identified, there are 200 actual bearing defects. In other words, the samples rejected at the first station include 16 defect-free bearings. This is because the system is calibrated more sensitive to detect the smallest rust defects. Specifically, 16 defect-free samples were excluded from mass production as they were classified as rust defect by the system. In addition, 2 impact, 1 scratch and 2 rust defects of the bearing samples with impact defect were not detected by the system and were not removed from production.

Table 5: Confusion matrix of the inspection results of the second inspection station.

Actual class	Predicted class				Number of samples
	Defect free	Impact	Scratch	Rust	
Defect free	184	0	0	16	200
Impact	2	38	0	18	58
Scratch	1	0	80	4	85
Rust	2	24	0	36	62
Total	189	62	80	74	405
Accuracy	$(184+38+80+36)/405 = 83.4\%$				

The third station ODIS is dedicated to inspect the outer diameter cylindrical surfaces of a bearing for visual defects. Referring to the inspection results as shown in Table 6, the third station inspected 277 samples, rejected 200 samples and allowed 62 samples to pass. There are 56 truly defect-free samples among the 62 passed samples. In other words, the third inspection station failed to reject 6 defective samples, including 2 impacts, 2 scratches, 2 rusts. It is worth noting that, 6 deformed samples that mistakenly passed the inspection. In addition, 6 defect-free bearings were mistakenly recognized as rust. Because the sensitivity of the rolling window is maximized so that even the smallest rust defects can be detected. However, this has even led to some defect-free samples being classified as defective. As a result, the accuracy of the third inspection station is 81.9%.

Table 6: Confusion matrix of the inspection results of the third inspection station.

Actual class	Predicted class					Number of samples
	Defect free	Impact	Scratch	Rust	Shoe trail mark	
Defect free	56	0	0	6	0	62
Impact	2	81	0	17	0	100
Scratch	2	0	45	0	0	47
Rust	2	12	0	30	0	44
Shoe trail mark	0	4	2	3	15	24
Total	62	97	47	56	15	277
Accuracy	$(56+75+45+23+15)/277 = 81.9\%$					

In fact, when we look at the system in general, our main goal is to catch the defect wherever it is found and to prevent this defective product from being sent to the customer. In this context, instead of classifying the defects according to their types, we can simply group all samples into two groups, OK or NG. The confusion

matrix of the results of the examination in two groups is shown in Table 7. As can be seen, the system did not reject eleven defective samples (false negative) and erroneously rejected ten perfect samples (false positive). When the overall accuracy rate of the system is considered, this ratio reaches a high value of 96.9%.

Table 7: Confusion matrix of all samples that categorized as either good or NG..

Actual class	Predicted class		Number of samples
	Good	NG	
Good	238	24	262
NG	13	897	910
Total	251	921	1172
Accuracy	$(238+897)/1172 = 96.8\%$		

CHAPTER 6

GENERAL CONCLUSION AND FUTURE WORKS

6.1. General Conclusion

The main purpose of this thesis is to examine the bearing surface non-destructively by image processing and to design a fully automated system to be used in mass production. The reason for its image processing based design is that all NDT techniques have been examined and it has been concluded that the most effective one among all techniques. Thus, VisiBear system design was started by evaluating all variations and requirements.

The first step of this thesis and the design of the VisiBear system is in chapter 2, first of all to define the bearing inspection zones precisely. In addition to defining the regions, the details of the visual defects in the respective regions are defined. Some of these details are related to the bearing to be inspected, while others are imposed by the industry or the customer. In addition, the advantages and disadvantages of the present visual quality control are described. Finally, it is aimed to overcome the current disadvantages with the developed VisiBear system and to reduce the workload of visual quality control workers in the first stage.

In Chapter 3, firstly, it is to examine all the researches on bearings in the literature. The aim of this study is to examine both theoretical studies and to see whether machine vision systems specific to bearings are made. However, as it is understood from the researches, it is observed that there is no visual defect detection system specific to the bearings and only the general purpose developed systems are tried to be adapted to the bearings. Although these systems are integrated into the bearings, they are only able to detect general defects and not very successful results on specific defects. This has revealed one of the main aims of this thesis. Secondly,

this section describes all the key elements for VisiBear and their properties. Thanks to these key points, a detailed discussion is provided for the proper selection of the necessary elements that will allow VisiBear to be designed from scratch. These key elements are cameras, lenses, lighting system and processing platform. Finally, a complete description of VisiBear system design and operating logic is presented. This system consists of a total of three cameras added to the fully automated production line of bearings. These cameras are sequenced sequentially according to the inspection zones of the inspected bearing, ensuring complete inspection of all visible surfaces of the customer.

In Chapter 4 and Chapter 5, this thesis involves the separation of bearing surfaces into different regions to detect visual defects, and the application and results of different statistical and morphological processes on all separated bearing regions. The first of these regions is the seal region and the surface is not homogeneous due to the embossed mark, resulting in an increase in the variety of methods to be applied. Firstly, for the types of defect of the reversely assembled rubber seal and missing rubber seal, the mean, STD, Variance, skewness and kurtosis parameters were calculated comparatively. In this comparative data, the variance value of missing rubber seal defect type is clearly differentiated. However, the distinction between the reversely assembled rubber seal and the defect-free bearing could not be achieved with these statistical calculations. The KLD and Power Graphs were then calculated, taking into account the fact that all the details are in the middle region of the seal, especially for the detection of reversely assembled rubber seal defects. CLD results were calculated comparatively over normal PDF and the distinction was achieved in a healthy way. In addition, in order to ensure a more accurate separation of the relevant visual defect, Power Graphics are also calculated in a comparative manner and 100% defect detection is achieved with KLD results. Since the overlap defect type, which is one of the defect types on seal region, is formed on the seal's lips designed for mounting the seal on the bearing, these lips are examined as a separate ROI from the Cartesian form. The homogeneous illumination of this type of defect has highlighted the structural defect of the seal lip. In this way, the defect is directly highlighted by converting it to a binary image. The overlap defect was detected in a healthy way with the Shifting / Rolling Window method. For

deformation and scratch defects on the seal, the middle region of the seal outside the lip parts of which the P2C transformed was selected as ROI. However, it is important and critical that there is an embossed mark in this selected ROI region and that this mark is not detected as a visual defect. More importantly, in some cases, the defect can occur on this embossed mark, and in this case it is extremely critical that the defect be detected precisely. At this stage, erosion / dilation methods were used locally to eliminate the embossed brand on the ROI via binary image. The selection of regionally different kernel sizes for Erosion / Dilation morphological processes has also enabled it to remain at the forefront of visual defects. Finally, deformation and scratch defects can be detected in a healthy way with Shifting / Rolling Window method. Secondly, there is a tendency to visual defects on the inner / outer rings from the bearing regions. One of the major disadvantages here is the scratches on the metal surface, which result from the characteristic grinding operation. These scratches are in the range of 200-225 nano meters and should not be perceived as defects. For this purpose, median filter was used primarily to remove grinding scratches on the surface. Then, Gaussian-Blur method was applied to make the surface more uniform and homogeneous, thus eliminating the characteristic scratches when the image was converted to binary image. Finally, Shifting / Rolling Window method determined different decision threshold values based on experience and scratch, rust and impact defects were determined precisely. Finally, visual defect checks were successfully performed on the cylindrical metal surface instead of the planar metal surface. The main disadvantage here was the problem of homogeneous illumination of the cylindrical surface. However, although this problem is tried to be solved by illumination, an irregular surface specific to illumination occurs at the edges due to the cylindrical structure. For this reason, irregularities were eliminated by cutting and resizing, and the maximum surface homogeneously illuminated as ROI was obtained. The characteristic grinding scratches described earlier, which are caused by the grinding process, are also present on the cylindrical metal surface. Therefore, the techniques applied on both the cylindrical surface and the planar metal surface are the same. The results of all mentioned statistical and morphological procedures are presented in Chapter 5 with details specific to the region and type of defect inspected.

Finally, again in Chapter 5, all methods applied and their results for defect detection and the accuracy percentages of the results obtained are examined on confusion matrices. First of all, these confusion matrices have been created by considering the classification according to different defect types encountered in different regions. As the types of defects that occur on the Rubber Seal are generally suitable and distinguishable types of defects for the classification process, the results have been verified with a high accuracy rate on RSIS, see Table 4. However, in the second station FIS, although rust and impact defects are detected during metal surface inspection, they may interfere with each other during defect classification. The main reason for this is that they are structurally very similar. The major difference of the impact defect from the rust defect is that it has a depth, not superficial. Since only one camera is used on station 2 in the designed VisiBear system, it is not possible to create depth perception and therefore there is confusion during classification. Although this reduces the percentage of accuracy slightly, the defective bearing detection is successfully performed, see Table 5. In addition, the rust defect on the metal surface can progress over time and reach the size to cover the entire surface. Therefore, it is one of the most critical and industrial conditions to detect the smallest rust defects. In the VisiBear system, the Shifting / Rolling Window size has been further reduced with experimental experience to detect rust defects. In this way, a more precise detection result is obtained for the detection of rust defects. However, in some cases, this precision causes defect-free bearings to be removed from production (due to the characteristic grinding scratches on them). This is completely lowering the profitability for the manufacturer. However, in addition to the guarantee that the defective bearing is not sent to the customer, it loses its importance. All false classification cases described for the second station are the same for the results of the third visual control station where the outer diameter surface is inspected, see Table 6. Finally, prevention of sending visual defective bearing to the customer is more important than classifying visual defects. In this context, instead of classifying the defects according to their types, we collected all samples simply in two groups as OK or NG. The overall accuracy percentage of the VisiBear system was 96.8% and a satisfactory level of overall performance was achieved, see Table 7.

6.2. Future Works

In order to be able to place the VisiBear system developed in this thesis to the serial production line, some capabilities need to be improved. In addition, to be integrated into the mass production line, the machine must be adapted to production standards. In order for the developed VisiBear to meet all these requirements, a number of enhancements are required, these are:

- In order to run all stations on the machine in automatic mode, the hybrid software created must be run on the PC side with thread commands. In this context, C ++ software will be translated into Object-Oriented Programming (OOP) architecture,
- PLC software is produced by the machine manufacturer R&S. So the software is built in Chinese and adding / changing is difficult or even impossible. As a result, the entire PLC software will be rebuilt in ORS,
- Trigger signal communication boards will be canceled (for conversion to voltage values of 2.4VDC - 24VDC or 24VDC - 2.4VDC). Instead of these cards, communication will be provided via Ethernet protocol Modbus TCP / IP,
- Graphic User Interface (GUI) design for general visualization of software running on image processing platforms and control of dynamic parameters of software.

REFERENCES

- [1] **Creusen, M. E., Schoormans, J. P. (2005).** The different roles of product appearance in consumer choice. *Journal of product innovation management*, 22(1), 63-81.
- [2] **ISO, I. (2005).**9000-Quality management systems–Fundamentals and vocabulary. Quality management systems, Berlin: BeuthVerlag GmbH, 22-25.
- [3] **Rollinson, D. (2008).**Organisationalbehaviour and analysis: An integrated approach. Pearson Education.
- [4] **Farago, F. T., Curtis, M. A. (1994).***Handbook of dimensional measurement.* Industrial Press Inc.
- [5] **Guerra, A. S., Pillet, M.,Maire, J. L. (2008).** Control of variability for man measurement.12th IMEKO TC1-TC7 joint Symposium on Man, France.
- [6] **Maire, J. L., Pillet, M., Baudet, N. (2013).** Gage r2&e2: an effective tool to improve the visual control of products. *International Journal of Quality & Reliability Management*, 30(2), 161-176.
- [7] **Kopardekar, P., Mital, A., Anand, S. (1993).** Manual, hybrid and automated inspection literature and current research. *Integrated Manufacturing Systems*, 4(1), 18-29.
- [8] **Workman G., (2012).***For Nondestructive Testing, Nondestructive Testing Overview*, Nondestructive testing handbook. American Society for Nondestructive Testing.
- [9] **Hellier C., (2012).***Handbook of Nondestructive Evaluation. Second Edition*, ser. Mechanical Engineering. McGraw-Hill Education.
- [10] Non-destructive testing: A guidebook for industrial management and quality control personnel,International Atomic Energy Agency (IAEA), Training Course, Jan. 1999.
- [11] **Zhang, B., Huang, W., Li, J., Zhao, C., Fan, S., Wu, J., Liu, C. (2014).** Principles, developments and applications of computer vision for external quality inspection of fruits and vegetables: A review. *Food Research*

International, 62, 326-343.

- [12] **Neogi, N., Mohanta, D. K., Dutta, P. K. (2014).** Review of vision-based steel surface inspection systems. *EURASIP Journal on Image and Video Processing*, 2014(1), 50.
- [13] **Shi, Y., Real, F. D. (2009).** Smart cameras: Fundamentals and classification. In *Smart Cameras* (pp. 19-34). Springer, Boston, MA.
- [14] **Ngan, H. Y., Pang, G. K., Yung, N. H. (2011).** Automated fabric defect detection—a review. *Image and vision computing*, 29(7), 442-458.
- [15] **Hanbay, K., Talu, M. F., Özgüven, Ö. F. (2016).** Fabric defect detection systems and methods—A systematic literature review. *Optik*, 127(24), 11960-11973.
- [16] **Norton-Wayne, L., Bradshaw, M., Jewell, A. J. (1992).** Machine vision inspection of web textile fabric. In *BMVC92* (pp. 217-226). Springer, London.
- [17] **Bradshaw, M. (1995).** The application of machine vision to the automated inspection of knitted fabrics. *Mechatronics*, 5(2-3), 233-243.
- [18] **Cho, C. S., Chung, B. M., Park, M. J. (2005).** Development of real-time vision-based fabric inspection system. *IEEE Transactions on Industrial Electronics*, 52(4), 1073-1079.
- [19] **Yang, Y., Miao, C., Li, X., Mei, X. (2014).** On-line conveyor belts inspection based on machine vision. *Optik-International Journal for Light and Electron Optics*, 125(19), 5803-5807.
- [20] **Fromme, C. C., Stager, D. J., Pilarski, T. E., Bancroft, B., Hegadorn, T. E. (2006).** *U.S. Patent No. 6,988,610*. Washington, DC: U.S. Patent and Trademark Office.
- [21] **Wei, T. (2010).** Research on detection technology for cracks of coal conveyor belt. *North University of China*, Taiyuan, 48-49.
- [22] **Neogi, N., Mohanta, D. K., Dutta, P. K. (2014).** Review of vision-based steel surface inspection systems. *EURASIP Journal on Image and Video Processing*, 2014(1), 50.
- [23] **Bigas, M., Cabruja, E., Forest, J., Salvi, J. (2006).** Review of CMOS image sensors. *Microelectronics journal*, 37(5), 433-451.

- [24] **Kempainen, S. (1997).** CMOS image sensors: eclipsing CCDs in visual information?.*EDN*, 42(21), 101-110.
- [25] **Hillebrand, M., Stevanovic, N., Hosticka, B. J., Conde, J. S., Teuner, A., Schwarz, M. (2000).** High speed camera system using a CMOS image sensor. *In Proceedings of the IEEE Intelligent Vehicles Symposium 2000 (Cat. No. 00TH8511)* (pp. 656-661). IEEE.
- [26] **Batchelor, B. G. (2012).***Selecting cameras for machine vision. Machine Vision Handbook*, London: Springer London, 2012, pp. 477-506.
- [27] **Martin, D. (2007).** A practical guide to machine vision lighting. *Retrieved*, 11(05), 2013.
- [28] **Batchelor, B. G. (2012).** Lighting-viewing methods. *Machine Vision Handbook*, 1345-1560.
- [29] **Batchelor, B. G. (2012).** Illumination sources, *Machine Vision Handbook. London: Springer London*, pp. 283-317.
- [30] **Bergin, T., Cusack, J., DeSmet, K. (2010).** Advantages of LED lighting in vision inspection systems. *QuadTech, Inc.*
- [31] **Narendran, N., Gu, Y. (2005).** Life of LED-based white light sources. *Journal of display technology*, 1(1), p.167.
- [32] **Birk, M., Zapf, M., Balzer, M., Ruitter, N., Becker, J. (2014).** A comprehensive comparison of gpu- and fpga-based acceleration of reflection image reconstruction for 3d ultrasound computer tomography, *Journal of Real- Time Image Processing*, vol. 9, no. 1, pp. 159-170.
- [33] **Gomez-Pulido J. A., Vega-Rodriguez, M. A., Sanchez-Perez, J. M., Priem-Mendes, S., Carreira, V. (2011).** Accelerating floating-point fitness functions in evolutionary algorithms: a FPGA-CPU-GPU performance comparison. *Genetic Programming and Evolvable Machines*, 12(4), 403-427.
- [34] **Kestur, S., Davis, J. D., Williams, O. (2010).** Blas comparison on fpga, cpu and gpu, *IEEE Computer Society Annual Symposium on VLSI*, pp. 288-293.
- [35] **Zou, D., Dou, Y., Xia, F. (2012).** Optimization schemes and performance evaluation of Smith–Waterman algorithm on CPU, GPU and FPGA. *Concurrency and Computation: Practice and Experience*, 24(14), pp. 1625-1644.

- [37] **Grozea, C., Bankovic, Z., Laskov, P. (2010).**FPGA vs. Multi-core CPUs vs. GPUs: Hands-On Experience with a Sorting Application, *Heidelberg: Springer Berlin Heidelberg*, pp. 105-117.
- [38] **Prakash, P., Blinka, E., Narnakaje, S., Friedmann, A., Garcia, K., Ferguson, R. (2016).** Multicore SoCs stay a step ahead of SoC FPGAs.
- [39] **Otsu, N. (1979).**A threshold selection method from gray-level histograms. *IEEE transactions on systems, man, and cybernetics*, 9(1), pp.62-66.
- [39] **Yusuf, M. D., Kusumanto, R. D., Oktarina, Y., Dewi, T., Risma, P. (2018).** BLOB Analysis for Fruit Recognition and Detection. *Computer Engineering and Applications Journal*, 7(1), 23-32.
- [40] **Jurie, F., Dhome, M. (2002, September).** Real Time Robust Template Matching. *In British Machine Vision Conference*, pp. 1-10.
- [41] **Vaquero, D., Turk, M., Pulli, K., Tico, M., Gelfand, N. (2010).** A survey of image retargeting techniques. *In Applications of Digital Image Processing XXXII,I* (Vol. 7798, p. 779814). International Society for Optics and Photonics.
- [42] **Deng, S., CAI, W., XU, Q., LIANG B (2010).** Defect detection of bearing surfaces based on machine vision technique, *International Conf. on Computer Application and System Modeling*, pp. 548-554.
- [43] **Chiou, Y. C., & Li, W. C. (2009).** Flaw detection of cylindrical surfaces in PU-packing by using machine vision technique. *Measurement*, 42(7), pp. 989-1000.
- [44] **Yuen, H. K.,Princen, J., Illingworth, J., Kittler, J. (1990).** Comparative study of Hough transform methods for circle finding. *Image and vision computing*, 8(1), pp.71-77.
- [45] **Nixon, M.,Aguado, A. S. (2012).***Feature extraction and image processing for computer vision*. Academic Press.
- [46] **Kumar, V., Gupta, P. (2012).** Importance of statistical measures in digital image processing. *International Journal of Emerging Technology and Advanced Engineering*, 2(8), pp.56-62.
- [47] **Soille, P. (2013).***Morphological image analysis: principles and applications*. Springer Science. pp. 65-68
- [48] **Gonzalez, R. C., & Woods, R. E. (2002).***Digital image processing*.

- [49] **Hershey, J. R., Olsen, P. A. (2007).** Approximating the Kullback-Leibler divergence between Gaussian mixture models. *In 2007 IEEE International Conference on Acoustics, Speech and Signal Processing-ICASSP'07*, Vol. 4, pp. IV-317
- [50] **Van Erven, T., Harremoës, P. (2014).** Rényi divergence and Kullback-Leibler divergence. *IEEE Transactions on Information Theory*, 60(7), pp. 3797-3820.
- [51] **Tsai, D. M., Chen, M. C., Li, W. C., & Chiu, W. Y. (2012).** A fast regularity measure for surface defect detection. *Machine Vision and applications*, 23(5), pp. 869-886.
- [52] **Mollaköy, A., Yengel, E., Töreyn, B. U. (2016).** Bearing fault detection method based on statistical analysis and KL distance. *In 2016 24th Signal Processing and Communication Application Conference (SIU)*, pp. 1881-1884.